scientific reports

Check for updates

OPEN

Translational readthrough therapy for ADPKD induces polycystin1 expression and partially rescues functional deficits in *PKD1* mutant cells

Elena Torban[1,2]✉, Lucie Canaff[3], Sima Babayeva[3], Nadezda Kachurina[3], Chen-Fang Chung[3], Albert C. M. Ong[4,5], Ahsan Alam[1] & Paul R. Goodyer[2,6]✉

Autosomal-Dominant Polycystic Kidney Disease, ADPKD, is the most common genetic kidney disease affecting 1:1000 people worldwide. It is caused by mutations in the *PKD1* (~80%) or *PKD2* gene (~15%). Although the germline mutation is inherited in dominant fashion, disabling the second allele is required for emergence of clonal cysts. Presently, no cure exists for ADPKD. In approximately 30% of patients, the heritable ADPKD mutation involves a single nucleotide substitution that converts the normal mRNA triplet encoding an amino acid into a Premature Termination Codon (PTC). The translation machinery poses at the PTC and detaches from the mutant mRNA; the unstable transcript and protein are degraded. Certain aminoglycosides bind to the mammalian ribosome and relax translational fidelity, permitting continued translation and production of a full-length protein. In this study, we tested the ability of aminoglycosides to induce readthrough of the PTC codons in the human *PKD1* gene and ascertained the effect of these drugs on pathologic features of *PKD1* mutant cells. We report that aminoglycosides induce 8–25% expression of full-length Polycystin1 (*PKD1* gene product) and significantly improve aberrant cell adhesion and cell signaling. Based on our observations, we propose that aminoglycoside readthrough drugs show potential as therapeutic agents for ADPKD.

Keywords Autosomal-dominant polycystic kidney disease, Readthrough drugs, Aminoglycosides, Premature termination codon, Therapy

Autosomal-dominant polycystic kidney disease, ADPKD, affects 1:1000 people worldwide and is inherited as a dominant trait associated with mutations in the Polycystic Kidney Disease gene 1, *PKD1* (~80%) or Polycystic Kidney Disease gene 2, *PKD2* (~15%), encoding two interacting proteins, Polycystin1 (PC1) and Polycystin2 (PC2)[1]. PC1 and PC2 are believed to form a receptor-Ca^{2+} channel complex that detects mechano- and chemo-external stimuli and transmits this information inside the cell to regulate key cell behaviors[2]. Both proteins are found at the primary cilium and elsewhere in renal epithelia[3,4]. Among those who inherit a germline mutation, somatic loss of the second allele disturbs the signals that normally constrain renal epithelial cell division to the tubular plane. Loss of polycystins disrupt signaling pathways that normally regulate cell proliferation, apoptosis, adhesion and motility, culminating in cyst formation. Progressive cyst enlargement over many years leads to renal failure between 40 and 70 years. Half of affected individuals develop end stage kidney disease by age 62, necessitating renal replacement therapy[5]. In addition, ADPKD often has extrarenal manifestations such as liver and pancreatic cysts[6] and vascular aneurisms[7], further increasing the social and financial burden on the patients and medical system.

For reasons that are unclear, about ~25% of germline *PKD1* gene mutations and ~40% of germline *PKD2* gene mutations involve a single nucleotide substitution that generates a Premature Termination Codon in the

[1]Division of Nephrology, Department of Medicine, Faculty of Medicine, McGill University, Montreal, QC, Canada. [2]McGill University Health Centre Research Institute, 1001 Boulevard Decarie, Block E, Room EM1.3248, Montreal, QC H4A3J1, Canada. [3]McGill University Health Centre Research Institute, Montreal, QC, Canada. [4]Division of Clinical Medicine, University of Sheffield Medical School, Sheffield, UK. [5]Sheffield Kidney Institute, Sheffield Teaching Hospitals NHS Foundation Trust, Sheffield, UK. [6]Department of Pediatrics, Faculty of Medicine, McGill University, Montreal, QC, Canada. ✉email: elena.torban@mcgill.ca; paul.goodyer@mcgill.ca

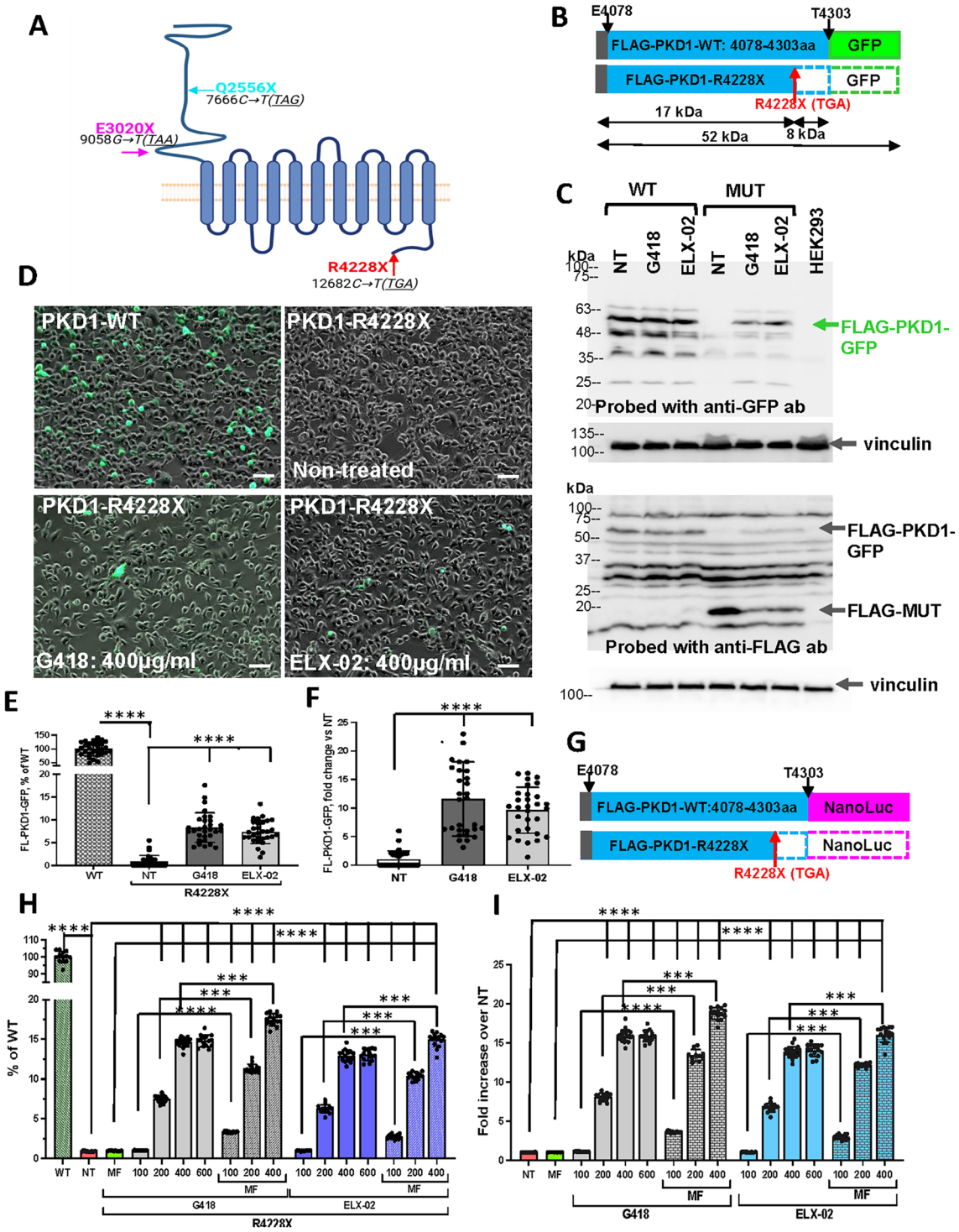

DNA (https://pkdb.mayo.edu). This is significantly higher than 10–12% prevalence of nonsense mutations in other genetic diseases[8]. In the corresponding mRNA, PTCs convert the normal nucleotide triplet that recognizes a transfer RNA delivering an amino acid to one of the three STOP codons, TAA, TAG and TGA, for which there are no cognate transfer mRNAs. When the translational machinery arrives at a STOP codon, translation comes to a halt, the dysfunctional truncated protein is released and both the unstable protein and its mRNA are usually degraded[9].

Remarkably, the impact of PTC can be modified by compounds belonging to the aminoglycoside family[10]. These drugs exert their antibiotic properties by binding to the bacterial ribosome and blocking protein translation. Although aminoglycosides bind only weakly to mammalian ribosomes and don't block mammalian protein translation, they do relax translational fidelity. This allows insertion of a "near-cognate" amino acid and completion of full-length protein synthesis[11]. The aminoglycoside G418 (geneticin) has shown to induce sufficient readthrough of certain PTCs to allow 5–20% of normal full-length protein synthesis[12,13]. Unfortunately, G418 is too toxic for use in clinical practice. Another aminoglycoside, gentamycin, is less toxic

◀**Fig. 1**. Aminoglycosides readthrough PKD1 reporters carrying R4228X mutation. (**A**) Schematic drawing of the human Polycystin1 protein. Position of each pathogenic variant investigated in this study is mapped, including the nucleotide and amino-acid changes. (**B**) Schematic drawing of the short PKD1 (amino acids 4078–4303) wildtype and R4228X reporters. eGFP tag is expressed at the C-terminus; FLAG tag is expressed at the N-terminus. The sizes of the full-length and truncated reporters are shown. (**C**) Western immunoblotting with anti-GFP antibody (upper panel) and anti-FLAG antibody (lower panel); each membrane was stripped and reprobed with anti-vinculin antibody. In the cells expressing FLAG-R4228X-eGFP reporter, eGFP tag is detected only upon treatment with G418 or ELX-02, while FLAG antibody allows to visualize wildtype and readthrough forms (52 kDa) and a shorter mutant form (17 kDa). (**D**) Both WT and R4228X reporters were expressed in the HEK293 cells and treated with 400 µg/ml G418 or ELX-02; cells expressing eGFP were identified on the overlay of the phase-contrast and fluorescence images; scale bar is 100 µm. (**E**,**F**) Statistical analysis of images in D presented as % of the eGFP-positive cells transfected with FLAG-PKD1-WT-eGFP and as a fold increase in the AMG treated over untreated cells expressing FLAG-PKD1-R4228X-eGFP construct. (**G**) Schematic drawing of the wildtype and R4228X reporters fused with NanoLuc gene at the C-terminus and FLAG tag at the N-terminus. Firefly Luciferase reporter was co-transfected with NanoLuc plasmids to monitor transfection efficiency. Nano-Glo® Dual-Luciferase® Reporter Assay was used to measure readthrough capacity of G418 and ELX-02 at various concentrations of aminoglycosides +/− mefloquine. (**H**) Statistical analysis of NanoLuc reporter experiments. The readthrough is presented as % of wildtype NanoLuc reporter expression. One-way Anova was used to compare untreated cells with the cells treated at all concentrations of AMG +/− MF, followed by the Tukey's multiple comparisons test. (**I**) The NanoLuc reporter activity is presented as the fold increase over untreated cells expressing FLAG-PKD1-R4228X-NanoLuc. Three independent experiments were carried out for each panel, each in triplicate, for each condition, except for (**B**), that was repeated twice. ***$p \le 0.001$; ****$p \le 0.0001$. NT—nontreated cells; MF—mefloquine.

and is commonly used in humans as an antibiotic for limited periods, but its readthrough properties are weak and may cause nephrotoxicity and ototoxicity in some individuals when given at higher doses or for prolonged periods[14,15]. Several laboratories have generated PTC readthrough drugs with a reduced toxicity profile[16,17]. Eloxx Pharmaceuticals developed a series of such aminoglycoside derivatives by screening for retention of PTC readthrough in mammalian cells, but diminished binding to the bacterial ribosome (a surrogate for toxicity at the related ribosomes in mammalian mitochondria)[18]**.** At a concentration of 5–7.5 µM, ELX-02 induced 2–22% translational readthrough in vitro for a variety of PTCs in the genes mutated in Hurler Syndrome, Cystic Fibrosis or Alport syndrome[12,19,20].

In this study, we show that G418 and ELX-02 induce translational readthrough of the three types of *PKD1* STOP codons reported in humans with ADPKD. This effect is substantially potentiated in the presence of mefloquine, an approved anti-malarial drug. We then examined the impact of these drugs on dysfunctional cellular pathways and show that this improves diminished adhesion and reduces excessive canonical WNT and YAP signaling in mutant *PKD1* cells. Our observations support the hypothesis that ELOX-02 may offer a potential therapeutic strategy for ADPKD.

Results

Over 250 germline STOP PTCs are listed in the ADPKD variant database (https://pkdb.mayo.edu). We selected several PTC variants for study (Fig. 1A): Q2556X (7666C>**T**, **TAG** stop codon), one of the most common PTC variants, maps to Exon 19; E3020X (9058**G**>**T, TAA** stop codon), maps to Exon 25; R4228X (12682**C**>**T**, **TGA** stop codon), the second most common PTC variant, maps to the very end of the PC1 protein in Exon 46. These three variants, representing the three known stop codons, were used to interrogate the efficacy of aminoglycoside-triggered translational readthrough of the human *PKD1* gene.

Aminoglycosides trigger translational readthrough of PTCs in human *PKD1* reporters

To ascertain whether aminoglycosides can readthrough STOP codons in the human *PKD1* gene, we first generated small wildtype human *PKD1* reporters that encode the C-terminus of the *PKD1* gene (amino acids 4078–4303), expressing either an eGFP or Nanoluc sequence fused in-frame at the C-terminus, as well as a FLAG epitope fused in-frame at the N-terminus of the construct (Fig. 1B,G). The R4228X variant (TGA stop codon) truncates the reporter so that the C-terminally positioned eGFP or Nanoluc signal could be detected only if the translational readthrough is triggered. After testing viability of HEK293 cells at various concentrations of G418 and ELX-02 (Supplemental Fig. 1A), eGFP/FLAG-tagged wildtype and mutant constructs were transiently expressed in the HEK293 cells and treated with 400 µg/ml G418 or 400 µg/ml ELX-02 for 40 h. Western immunoblotting with anti-eGFP antibody detected an eGFP signal in the cells expressing R4228X reporter only after treatment with G418 but not without treatment (Fig. 1C, upper panel). Wildtype protein was robustly expressed at the same levels with or without treatment (Fig. 1C). In the absence of aminoglycosides, only ~ 17 kDa band corresponding to the truncated FLAG-PKD1-R4228X (FLAG-MUT) protein could be detected with the anti-FLAG antibody (Fig. 1C, lower panel probed with ani-FLAG antibody). Treatment of the cells expressing a mutant reporter with 400 µg/ml G418 or ELX-02 revealed a ~ 52 kDa band, that corresponds to the size of the FLAG-PKD1-WT-GFP protein (Fig. 1C, lower panel probed with ani-FLAG antibody). All original uncropped blots are shown in Supplemental Fig. 12. The eGFP-positive signal was visualized in live cells using an overlay of the phase-contrast and fluorescence channels (Fig. 1D). The number of FLAG-R4228X-eGFP-positive cells was normalized to the number of eGFP+ cells expressing wildtype FLAG-PKD1-eGFP reporter (% of wildtype expression) or to the non-treated cells expressing FLAG-PKD1-R4228X-eGFP reporter (fold increase). Both 400 µg/ml G418 and

400 µg/ml ELX-02 triggered PTC readthrough on average ~ 8% (G418) and ~ 7% (ELX-02) of wildtype reporter expression. When normalized for eGFP expression in non-treated cells, 400 µg/ml G418 induced a ~ 12-fold increase in the eGFP+ signal whereas ELX-02 efficacy was a bit lower, triggering ~ ninefold increase in the cells expressing FLAG-PKD1-R4228X-eGFP protein (Fig. 1E,F).

Cells transfected with FLAG-PKD1-WT-Nanoluc and FLAG-PKD1-R4228X-Nanoluc were treated for 40 h with 100–600 µg/ml of either G418 or ELX-02 (Fig. 1H,I). The treatment induced a concentration-dependent increase in the readthrough activity, reaching ~ 17% (G418) and ~ 14% (ELX-02) of the FLAG-PKD1-WT-Nanoluc expression levels at 600 µg/ml concentration. Compared to the untreated cells, treatment with 600 µg/ml G418 or ELX-02 triggered a 17-fold (G418) and 15-fold (ELX-02) increase in the NanoLuc signal.

Several molecules that enhance readthrough activity of aminoglycosides have been described, including the anti-malarial drug mefloquine (approved for human use)[13]. Using the FLAG-PKD1-R4228X-Nanoluc reporter, we observed significant enhancement of readthrough with mefloquine in combination with an aminoglycoside. Although mefloquine alone had no appreciable effect (Fig. 1H,I), 7.5 µM mefloquine added to 100–00 µg/ml G418 or 100–400 µg/ml ELX-02, enhanced readthrough to ~ 19% (G418) and ~ 18% (ELX-02) of wildtype expression (Fig. 1H). Similarly, 7.5 µM mefloquine enhanced G418 readthrough 20-fold and ELX-02 18-fold, when compared to the level in untreated cells (Fig. 1I). Importantly, mefloquine significantly enhanced PTC readthrough at all concentrations of each aminoglycoside (Fig. 1I).

Next, we studied translation in the context of the full-length *PKD1* transcript (encoding amino acids 1–4303), reasoning that elements other than the STOP codon sequence itself might influence aminoglycoside-induced readthrough. HEK293 cells were stably transfected with a human full-length wildtype *PKD1* construct fused in-frame with a FLAG tag at the C-terminus (PKD1-WT-FLAG) or the corresponding mutant *PKD1* construct bearing a TAA PTC (PKD1-E3020X-FLAG) (Fig. 2A). The cells were then treated with 400 µg/ml G418 or 400 µg/ml ELX-02 for 48 h. On Western immunoblots probed with an anti-FLAG antibody, full-length Polycystin1 band (~ 450–500 kDa) was detected in cells expressing PKD1-WT-FLAG and PKD1-E3020X-FLAG cells after G418 or ELX-02 treatment but not in the untreated PKD1-E3020X-FLAG cells (Fig. 2B). When the cells overexpressing PKD1-WT-FLAG cDNA were analyzed with a well-characterized N-terminus anti-Polycystin-1 antibody 7e12[21], an upper PC1 band (~ 450–500 kDa) and a lower PC1 band (~ 320 kDa) could be seen (Fig. 2 and Supplemental Fig. 2). The upper band corresponds to the full-length Polycystin1 protein. The lower band likely corresponds to the PC1 protein that is proteolytically cleaved within the GPS tripeptide His-Leu-*Thr3048 site, generating a large N-terminal PC1 fragment, NTF (~ 320 kDa)[22]. A smaller C-terminus PC1 fragment, CTF (~ 130 kDa) is also generated as a result of proteolytic cleavage at amino acid 3048. We detected CTF in the cells expressing wildtype reporter or in the treated cells expressing mutant reporter, when probed with anti-FLAG antibody (Fig. 2B). Untreated PKD1-E3020X-FLAG-expressing clones showed only the mutant truncated protein (running at the same size as the proteolytically-cleaved form in the cells expressing PKD1-WT-FLAG cDNA (Fig. 2C). Endogenous expression of the PC1 protein in the HEK293 cells was undetectable with the 7e12 antibody (Supplemental Fig. 2). In two independent HEK293/PKD1-E3020X-FLAG clones, aminoglycosides induced significant expression of full-length PC1 (PC1-FL band): 400 µg/ml G418 triggered readthrough at ~ 25% (clone A) and ~ 27% (Clone B) of that in cells expressing PKD1-WT-FLAG construct; ~ 50-fold increase (clone A) and up to 55-fold increase (clone B) compared to the untreated PKD1-E3020X-FLAG clones. The efficacy of 400 µg/ml ELX-02 was slightly lower yet still highly significant: ~ 21% (clone A) and ~ 22% (clone B) relative to the wildtype Polycystin1 expression and ~ 40-fold (clone A) and ~ 50-fold (clone B) increase compared to the untreated HEK293 clones expressing PKD1-E3020X-FLAG cDNA.

Stability of the readthrough of PC1-FL in PKD1-E3020X-expressing cells was evaluated by treating the cells with 400 µg/ml G418 or 400 µg/ml ELX-02 for 48 h and then allowing a drug-free "wash-out" period for additional 48 h (96 h total from the start of treatment) (Fig. 3 A, B). The PC1-FL could be detected up to 96 h in PKD1-E3020X cells treated with either aminoglycoside (Fig. 3A–D).

Aminoglycosides trigger translational readthrough of PC1 in patient-derived *PKD1* cyst cells

The WT9-12 cell line was previously established from the epithelial lining of a renal cyst in a female ADPKD patient. These cells bear a Q2556X mutation (TAG stop codon) on one allele in combination with a somatic deletion of the trans-allele[23] (Fig. 4A). WT9-12 cells were treated for 48 h with non-toxic concentration 400 µg/ml G418 or 400 µg/ml ELX-02 in the presence or absence of 5 µM mefloquine (Supplemental Fig. 1B). RT-qPCR analysis indicates that treatment with either G418 or ELX-02 increases *PKD1* transcript levels (amplified with two independent sets of primers) (Fig. 4B). The levels of *PKD1* mRNA were unchanged in the presence of mefloquine alone. However, addition of 5 µM mefloquine to aminoglycosides increased *PKD1* mRNA levels ~ fivefold (G418) and ~ fourfold (ELX-02) comparing to the untreated cells (Fig. 4B).

In WT9-12 cells, the full-length PC1 protein is undetectable, yet a faint ~ 280 kDa band can be seen with 7e12 antibody (Fig. 4C). This band likely corresponds to the mutant truncated PC1-Q2556X protein. At a concentration of 200 µg/ml neither aminoglycoside induced sufficient readthrough to detect full-length Polycystin-1 (Fig. 4C). However, at 400 µg/ml, modest translational readthrough was seen: ~ 5–6% (G418) and ~ 3% (ELX-02) of endogenous full length PC1 in normal control (HK-2) cells used as a control (Fig. 4D). 5 µM mefloquine alone had no effect but nearly doubled levels of Polycystin1 in combination with 400 µg/ml G418 or ELX-02 (Fig. 4D).

Polycystin1 is proteolytically cleaved at amino acid 3048, generating a large N-terminal PC1 fragment, NTF (~ 320 kDa); when glycosylated, it can acquire a higher molecular weight of ~ 400–450 kDa and visualized alongside full-length PC1 protein[22,24]. In addition, endogenous human *PKD1* transcript is frequently differentially spliced over introns 21 and 22, generating a major alternatively spliced truncated ~ 330 kDa isoform (PC1-AT)[24]. However, the Q2556X mutation maps to exon 19. Therefore, without readthrough of the upstream Q2556X PTC, neither full-length, nor N-terminal fragment or alternatively spliced truncated PC1 protein can be generated.

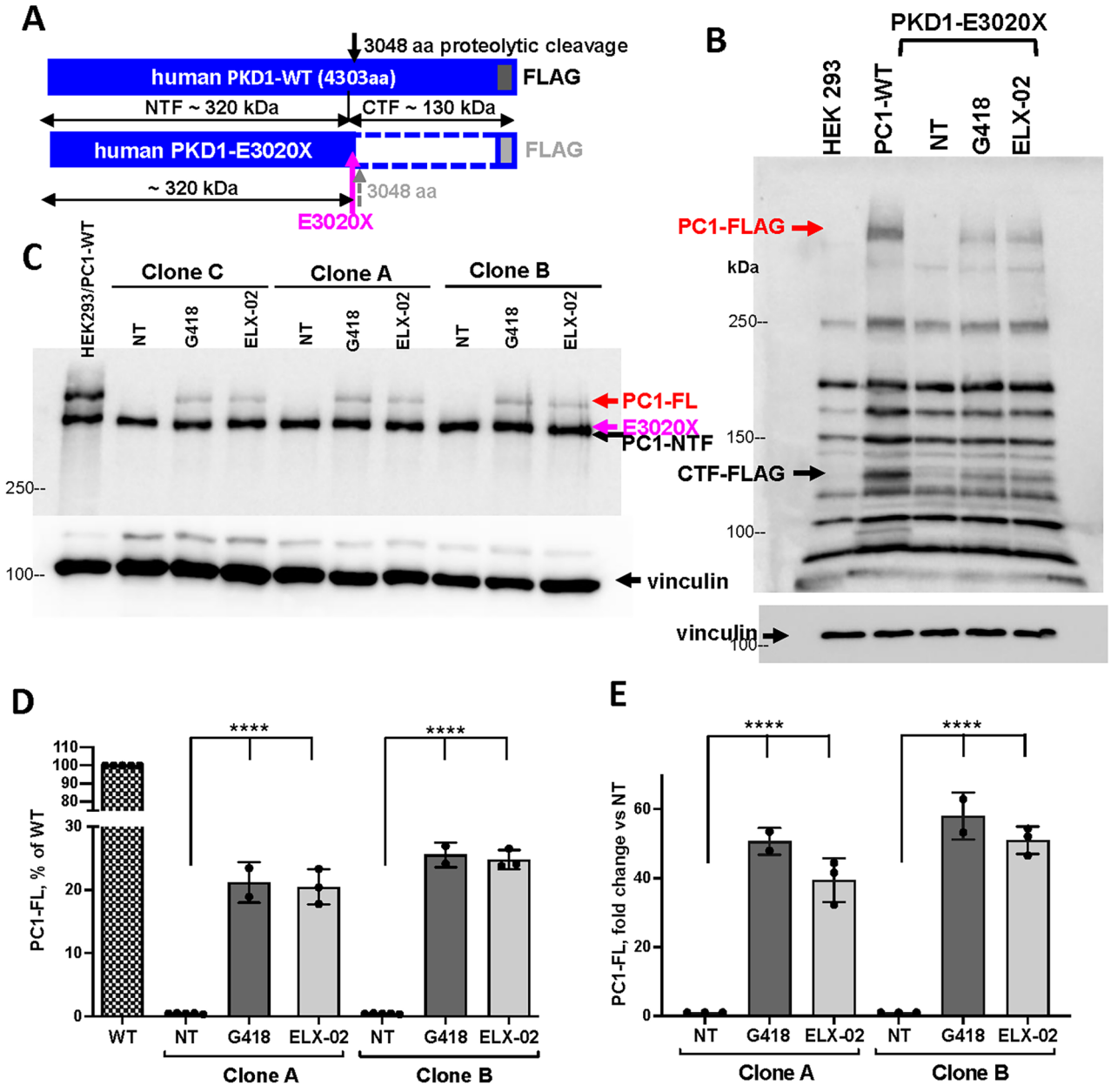

Fig. 2. Aminoglycoside-mediated PTC readthrough of PKD1-E3020X pathogenic variant in the stably-transfected HEK293 cells. (**A**) Schematic drawing of the wildtype PKD1-WT-FLAG and PKD1-E3020X-FLAG expression constructs. Both constructs express FLAG tag at the C-terminus however, in the PKD1-E3020X-FLAG construct, FLAG can be expressed only upon successful PTC readthrough. Note that PC1 protein is proteolytically cleaved at amino acid 3048 and two fragments are generated: ~ 320 kDa N-terminal fragment, NTF, and ~ 130 kDa C-terminal fragment, CTF. (**B**) Both PKD1-WT-FLAG and PKD-E3020X-FLAG constructs were stably expressed in the HEK293 cells, and immunodetection with anti-FLAG antibody was carried out. Full-length PC1 or CTF bands are detected in the cells expressing PKD1-WT-FLAG and only upon treatment of PKD1-E3020X-FLAG-expressing cells with 400 µg/ml G418 or ELX-02. (**C**) Western immunodetection of PC1 with 7e12 antibody. WT Lane: HEK293 cells stably expressing PKD1-WT-FLAG cDNA. Both the full-length PC1 (PC1-FL, upper band) and a ~ 320 kDa N-terminal fragment (PC1-NTF) can be detected. HEK293 cells transfected with PKD1-E3020X – three individual clones (clones A, B, C); a strong band that corresponds to the PC1-E3020X is visible. Upon treatment with 400 µg/ml of either G418 or ELX-02 for 48 h, the PC1-FL (upper band) can be visualized. (**D**) Densitometric intensity of bands corresponding to PL1-FL was measured on membranes from three independent experiments, normalized for vinculin expression and shown as % of wildtype PC1-FL. (**E**) PC1-FL levels in the presence of aminoglycoside are presented as fold increase compared to the untreated cells expressing PC1-E3020X. Three independent experiments were carried out. ****$p \leq 0.0001$ (one-way ANOVA) followed by the Tukey's multiple comparisons test. NT- nontreated cells.

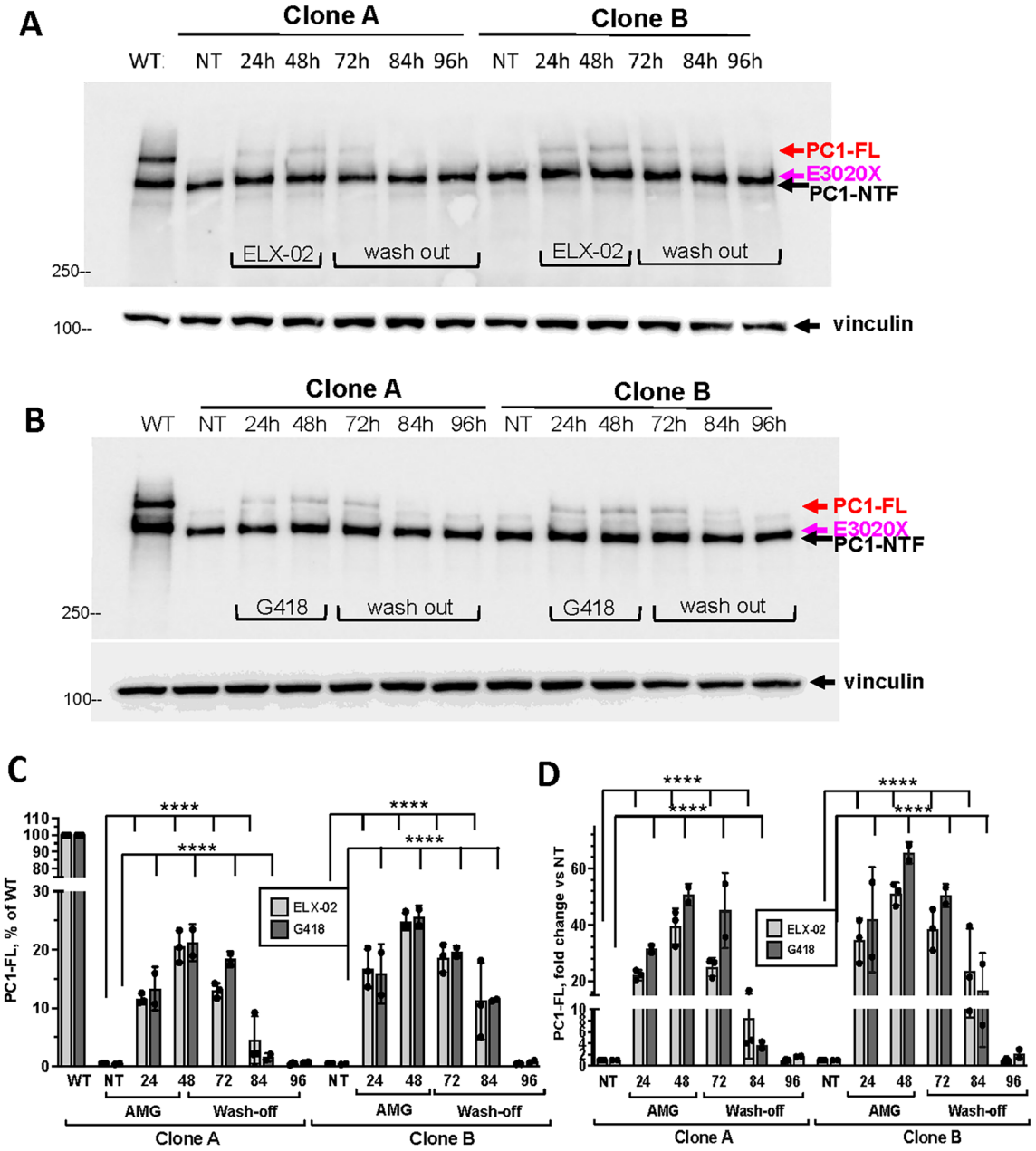

Fig. 3. Stability of AMG-mediated PC1 readthrough in the HEK293 clones expressing PKD1-E3020X pathogenic variant. (**A**) HEK293 cells stably expressing truncated PC1-E3020X protein seen as a lower band (clones A and B) were treated with 400 µg/ml ELX-02 for 48 h. After 48 h, cells were washed and collected at 72, 84 or 96 h after start of the treatment. WT lane shows HEK293 cells stably overexpressing PC1-WT-FLAG protein. (**B**) The clones were treated with 400 µg/ml G418 for the same duration followed by a wash-ff regimen. (**C**) Densitometric intensity was measured on Western blot membranes from three independent experiments for each AMG treatment. The intensity of the upper PC1-FL band was normalized for vinculin and presented as % of wildtype PC1-FL band intensity (assigned 100% value). (**D**) The densitometric data presented as fold increase in expression of PC1-FL from the mutant E3020X transcript vs non-treated cells. Three independent experiments were carried out. ****$p \leq 0.0001$ all treated lanes vs no treatment (NT), one-way Anova followed by the Tukey's multiple comparisons test. NT- nontreated cells.

Therefore, we calculated AMG readthrough activity based on the combined intensity of PC1-FL (~450 kDa) and the PC1-PC & PC1-AT (320–330 kDa) proteins (PC1-total) in the treated WT9-12 cells relative to the intensity of the PC1-total bands seen in the HK-2 cells. Without mefloquine, only ~ 2–4% of PC1-total readthrough was detected, however, 5 µM mefloquine enhanced readthrough of the Q2556X to ~ 8.5% (400 µg/ml G418 + MF) and ~ 6% (400 µg/ml ELX-02 + MF) of the level in HK-2 cells (Fig. 4E).

To evaluate stability of the full-length, NTF and alternatively spliced PC1 products induced by aminoglycoside with or without mefloquine in WT9-12 cells, the cells were treated with aminoglycosides for 48 h and then incubated in fresh medium for additional 48 h. The newly synthesized PC1-FL and PC1-NTF/PC1-AT bands were detected for up to 84 h from the start of the experiment (Fig. 5A–D).

Aminoglycosides rescue adhesion in cells expressing STOP codons

Mutant *PKD1* epithelial cells exhibit altered adhesiveness to various substrates in vitro[25,26]. To ascertain whether this ADPKD phenotype could be rescued, we measured adhesion of the HEK293 cells stably expressing similar levels of full-length PKD1-WT-FLAG or PKD1-E3020X-FLAG cDNA. The clones expressing mutant *PKD1* construct exhibited on average ~ 18% weaker adhesion to the collagen type I-coated surface compared to the cells expressing wildtype *PKD1* construct (Fig. 6A). Treatment of HEK293/PKD1-E3020X cells with aminoglycosides (400 µg/ml) increased cell adhesion modestly but significantly (Fig. 6A). Aminoglycosides did not affect HEK293/PKD1-WT-FLAG cell adhesion (Supplemental Fig. 3A).

To test whether adhesion of mutant WT9-12 cells differs from cells expressing wildtype *PKD1*, we generated clones of WT9-12 cells stably expressing a wildtype PKD1-WT-FLAG construct. Two clones with exogenous PC1 expression levels similar to that in HK-2 cells were chosen for further experiments (Supplemental Fig. 4). Adhesion of WT9-12 cells was ~ 25% weaker than that of the two independent WT9-12/PKD1-WT-FLAG clones. Treatment of WT9-12 cells with 400 µg/ml aminoglycosides significantly improved cell adhesiveness, though the effect was modest (Fig. 6B). Aminoglycosides had no effect on adhesion of WT9-12/PKD1-WT-FLAG cells (Supplemental Fig. 3B).

Expression of the β1-integrin transcript (*ITGB1* gene) and the corresponding protein has been reported by others to be altered in cells with loss of *PKD1*[27–29]. Therefore, we compared the expression of *ITGB1* mRNA by RT-qPCR in stable HEK293 clones expressing either PKD1-WT-FLAG or PKD1-E3020X-FLAG. *ITGB1* mRNA expression was significantly decreased in PKD1-E3020X-expressing clones compared to PKD1-WT-FLAG-expressing cells (Fig. 6C). Importantly, the levels of *ITGB1* mRNA in HEK293/E3020X-expressng cells treated with 400 µg/ml of G418 or ELX-02 were increased, in parallel with a modest increase in adhesion of these cells upon treatment (Fig. 6C). Similarly, we detected a significant decrease of *ITGB1* mRNA level in mutant WT9-12 cells compared to basal *ITGB1* transcript in WT9-12/PKD1-WT-FLAG control cells (Fig. 6D). Incubation of WT9-12 cells with aminoglycosides led to an increase in *ITGB1* mRNA expression that was further potentiated by addition of mefloquine (Fig. 6D).

Polycystin 1 is a large transmembrane protein localized at the plasma membrane and primary cilium[3,30]. It is known to precipitate with the adhesion complex components and influence adhesion[26,31]. Therefore, if the improvement in cell adhesion in aminoglycoside-treated mutant cells is due to readthrough of Polycystin 1, then the readthrough protein should be expressed at the cell surface. To test this, we performed a surface biotinylation assay to determine whether readthrough PC1 protein translated from the mutant Q2556X allele in the patient-derived WT9-12 cells could reach the plasma membrane (see Supplemental Fig. 5). As expected, the full-length and N-terminal forms of wildtype PC1 in control WT9-12/PKD1 cells were biotinylated, pulled down on NeutrAvidin agarose beads and detected by Western blotting using the 7e12 antibody. Importantly, we also detected biotinylated readthrough full-length and N-terminal PC1 forms (Supplemental Fig. 5), suggesting that readthrough PC1 is likely to be functional.

Aminoglycosides rescue WNT and YAP signaling in patient-derived cells

Kidney cyst growth and progression in ADPKD has been associated with deregulation of multiple signaling pathways[32], including canonical WNT signaling[33,34] and YAP signaling[35,36]. We used a well-characterized TOPFLASH assay, where a Luciferase reporter is expressed under control of a canonical WNT-sensitive promoter[37]. The HEK293 clones expressing PKD1-WT-FLAG and PKD1-E3020X-FLAG constructs were transiently transfected with TOPFLASH reporter and stimulated with either L-WNT3a or L-cell conditioned medium. The HEK293/PKD1-E3020X clones were ~ 65% more responsive to WNT3a than HEK293 cells expressing PKD1-WT-FLAG (Fig. 7A). Cells transfected with FOPLASH, a reporter in which WNT-sensitive motif is mutated, did not respond to WNT3a stimulation (Supplemental Fig. 6). When treated with either 400 µg/ml G418 or ELX-02, TOPLASH-Luciferase activity decreased modestly but significantly to the 152–155% range compared to PKD1-WT-FLAG-expressing cells. G418 had a more pronounced effect than ELX-02 (Fig. 7A). Aminoglycoside treatment of HEK293 clones expressing wildtype PKD1 had no effect on WNT signaling (Supplemental Fig. 7A). The WNT activity in WT9-12 cells was ~ 35% higher compared to WT9-12/PKD1-WT-FLAG clones (Fig. 7B). Cell treatment with 400 µg/ml G418 or ELX-02, especially in combination with 5 µm mefloquine, significantly reduced WNT signaling to about 120% of that seen in WT9-12/PKD1-WT-FLAG clones. We detected no change in WNT activity for WT9-12/PKD1-WT-FLAG cells exposed to aminoglycosides with or without mefloquine (Supplemental Fig. 7B).

Canonical WNT signaling is mediated by β-catenin, which is stabilized in cytoplasm and translocates from cytoplasm to the nucleus in response to canonical WNT signals (reviewed in[38]). Therefore, we measured both total and nuclear intensity of β-catenin detected by immunofluorescence microscopy. There was a significant increase in the signal intensity corresponding to the total and nuclear localization of β-catenin in untreated mutant WT9-12 cells versus WT9-12/PKD1-WT-FLAG cells (Fig. 7C–E; Supplemental Fig. 8). This increase was modestly but significantly reduced after WT9-12 cell treatment with 400 µg/ml PTC-readthrough drugs and 5 µm mefloquine (Fig. 7C–E; Supplemental Fig. 8).

Elevated nuclear retention of the Yes-associated protein, YAP (a downstream mediator of the Hippo pathway) has been associated with ADPKD pathogenesis[35,36]. Thus, we explored the subcellular localization of YAP in the mutant WT9-12 and WT9-12/PKD1-WT-FLAG cells by immunofluorescent microscopy with anti-YAP1 antibody (Fig. 8A; Supplemental Fig. 9). We found a highly significant increase in the nucleus:cytoplasm ratio

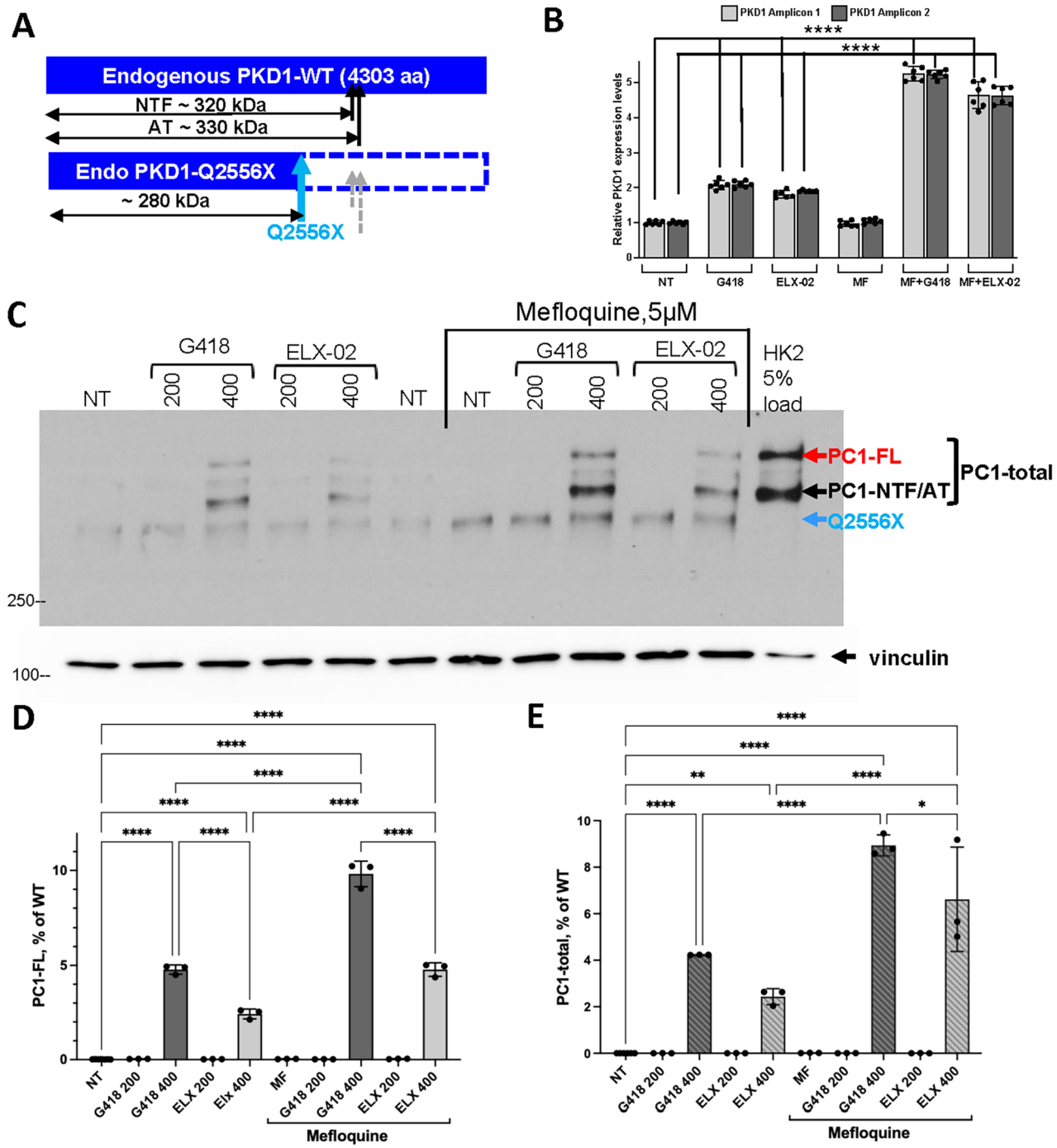

of YAP expression in mutant cells (Fig. 8B). This ratio was significantly reduced in mutant cells after treatment with 400 μg/ml of an AMG in combination with 5 μM mefloquine (Fig. 8B). We validated these results by using a YAP-Luciferase reporter, which reflects YAP transcriptional activity[39]. As shown in Fig. 8C, YAP reporter activity in mutant cells was on average ~ 75% higher compared with the WT9-12/PKD1-WT-FLAG cells. YAP activity decreased significantly in WT9-12 cells treated with 400 μg/ml G418 or ELX-02 (Fig. 8C); further decrease in YAP reporter activity was noted when 5 μm mefloquine was added to an aminoglycoside (Fig. 8C). AMG treatment of WT9-12 cells expressing wildtype PKD1 cDNA did not affect YAP-Luciferase activity (Supplemental Fig. 10). To validate YAP-luciferase reporter results, we analyzed expression of several well-characterized YAP transcriptional targets (See Supplemental Table). For 7 out of 8 interrogated target genes, expression in the WT9-12 cells was significantly elevated comparing to the control WT9-12/PKD1-WT-FLAG cells. Cell treatment with 400 μg/ml G418 and ELX-02 decreased YAP gene expression, which was further potentiated in the presence of 5 μM mefloquine (Fig. 8D).

Discussion

In this study, we demonstrate that aminoglycosides induce significant translational readthrough of human *PKD1* mRNA bearing a STOP codon, allowing production of full-length Polycystin1. The restoration of *PKD1*

◀**Fig. 4**. Aminoglycoside-mediated readthrough of the endogenous human *PKD1*-Q2556X pathogenic variant in the patient-derived cells. (**A**) Schematic drawing of the endogenous *PKD1*-Q2556X allele in the WT9-12 cells (ATCC); the size of the Q2556X band is ~ 280 kDa; the NTF is ~ 320 kDa; the alternatively spliced truncated form (AT) is ~ 330 kDa. (**B**) qRT-PCR of the PKD1 mRNA expression in the WT9-12 cells treated with aminoglycosides +/− 5 μM mefloquine (MF). Two pairs of primers to amplify two non-overlapping amplicons were used. Three independent experiments were done in duplicate for each condition. (**C**) WT9-12 cells do not express detectable PC1 full length (PC1-FL), nor they express a proteolytically cleaved N-terminal fragment (PC1-NTF) or a major alternatively spliced truncated form (PC1-AT). However, a weak band of ~ 280 kDa is detectable that likely corresponds to the truncated PC1- Q2556X protein. WT lane shows PC1 expression in the established HK-2 proximal tubular cells (5% cell lysate was loaded into the WT lane). Note absence of the Q2556X truncated PC1 form in the HK-2 lane. (**D**) Densitometric intensity of the full-length PC1 band (upper PC1-FL) was measured in three independent experiments, and each intensity value was normalized for a corresponding vinculin expression (loading control). The PC1-FL expression in the WT9-12 cells is plotted as % of the PC1-FL expression in the wildtype cells. (**E**) Densitometric intensity of the total PC1 expression (combined intensities of PC1-FL, proteolytically cleaved N-terminal fragment PC1-NTF and alternatively spliced truncated form PC1-AT) was measured, normalized for a corresponding vinculin level (loading control), and presented as % of the PC1-total expression in the HK-2 cells. Note, endogenous PC1-NTF and PC1-AT proteins are of similar molecular weight (~ 320–330 kDa) and cannot be distinguished under the conditions used. Three independent experiments were carried out. *$p \le 0.05$, **$p \le 0.01$, ****$p \le 0.0001$ (one-way ANOVA) followed by the Tukey's multiple comparisons test. NT—nontreated cells; MF—mefloquine.

expression is associated with improvement in cell adhesion and inhibition of excessive canonical WNT and YAP signaling. Based on these observations, we propose that aminoglycosides, especially with mefloquine, constitute a way to reverse key pathogenic mechanisms underlying ADPKD and might offer a novel therapeutic strategy with the potential to improve disease outcome.

G418 is known to induce translational readthrough of mRNA STOP codons[12,13]. However, its use in clinical practice is precluded by significant toxicity in mitochondrion-rich tissues such as kidney. For that reason, ELX-02 was developed by screening aminoglycoside derivatives for good readthrough of mammalian PTCs but reduced binding to the bacterial ribosome—a surrogate for mammalian mitochondrial toxicity[17]. The improved readthrough/toxicity profile of ELX-02 led to FDA authorization of several clinical trials: NCT04126473 in cystic fibrosis (Phase 2); NCT04069260 in Cystinosis (Phase 2); NCT05448755 in Alport syndrome (Phase 2). In our study, the readthrough effect of ELX-02 for each of the three types of STOP codons was somewhat lower than that of G418. Nevertheless, it consistently induced Polycystin1 expression ranging from 5 to 20% of wildtype PKD1 expression, depending on the assay in which the STOP codon was tested and the cell type used.

Aminoglycosides are thought to enhance incorporation of near-cognate transfer RNAs at STOP codons by binding directly to the decoding center of the 80S ribosome that links transfer RNA to the mRNA codon[40]. Ferguson et al. reported that mefloquine, an oral drug approved for malarial prophylaxis, could enhance the readthrough effects of aminoglycosides, though it had no readthrough effects on its own[13]. Using X-ray crystallography and single-particle cryo-EM, it was recently shown that mefloquine, in a complex with G418, binds directly to the proteins of translation machinery in the inter-subunit space of the ribosomal decoding center, changing the rotational state of the vacant ribosome[40], thereby facilitating PTC readthrough. Indeed, in our study, in combination with both G418 and ELX-02, mefloquine significantly potentiated AMG efficacy of *PKD1* PTC readthrough. This was particularly noticeable in the patient-derived WT9-12 cells bearing mono-allelic Q2556X PTC: treatment with both mefloquine and AMGs increased synthesis of full-length Polycystin1 by almost 100%. Moreover, the availability of the *PKD1* mRNA increased fivefold compared to untreated cells, as detected by qRT-PCR. By inducing readthrough activity, AMGs may interfere with nonsense mRNA-mediated decay (NMD), the cellular surveillance mechanism that identifies mRNAs containing PTCs and degrades them[41]. Our in silico analysis of the Q2556X mutations using NMDetective algorithms[42] indicates that Q2556X allele is highly NMD-susceptible (Supplemental Fig. 11), however, mefloquine alone did not increase either *PKD1* mRNA or PC1 protein levels. Thus, it is likely that enhancement of Q2556X readthrough upon treatment with both mefloquine and AMGs is due to their combined effects on the ribosome/translational machinery complex.

Although ADPKD is inherited as a dominant condition, it behaves as a recessive genetic disease at the cellular level. While heterozygous germline PTCs don't have an overt effect on renal tubular morphology, loss of the second allele through random sporadic mutations during tubular cell division is thought to give rise to clonal cysts[43,44]. In a recent study, kidney organoids carrying heterozygous *PKD1* or *PKD2* nonsense mutations did not develop cysts, whereas > 75% of organoids carrying the same mutations in homozygosity were cystic[45]. Notably, experimental repair of one mutant allele with CRISPR/Cas9 technology rescued cystogenesis ex vivo[45]. Hence, PC1 or PC2 expression levels must dip well below the 50% mark to drive cyst formation. A frequently occurring abnormal alternative splicing of human *PKD1* mRNA produces a much shorter (~ 330 kDa), primarily endoplasmic reticulum-residing, dysfunctional truncated PC1 form. This is believed to further reduce the overall levels of functional PC1, thereby increasing the risk of cyst formation[24]. In some recessive genetic diseases such as cystinosis, residual expression of the CTNS protein as low as 10% of the wildtype averts kidney failure and leads only to a mild ocular phenotype[46]. Thus, it is reasonable to postulate that aminoglycoside readthrough of *PKD1* STOP codons, permitting Polycystin1 expression in the range of 10% of wildtype cells, might be sufficient to prevent cystogenesis or slow down the rate of cyst growth over time. If so, it is conceivable that long-term use of a non-toxic aminoglycoside +/- mefloquine might improve renal outcome in the subgroup of ADPKD patients (about one third) who inherit a PTC variant of the *PKD1* or *PKD2* gene.

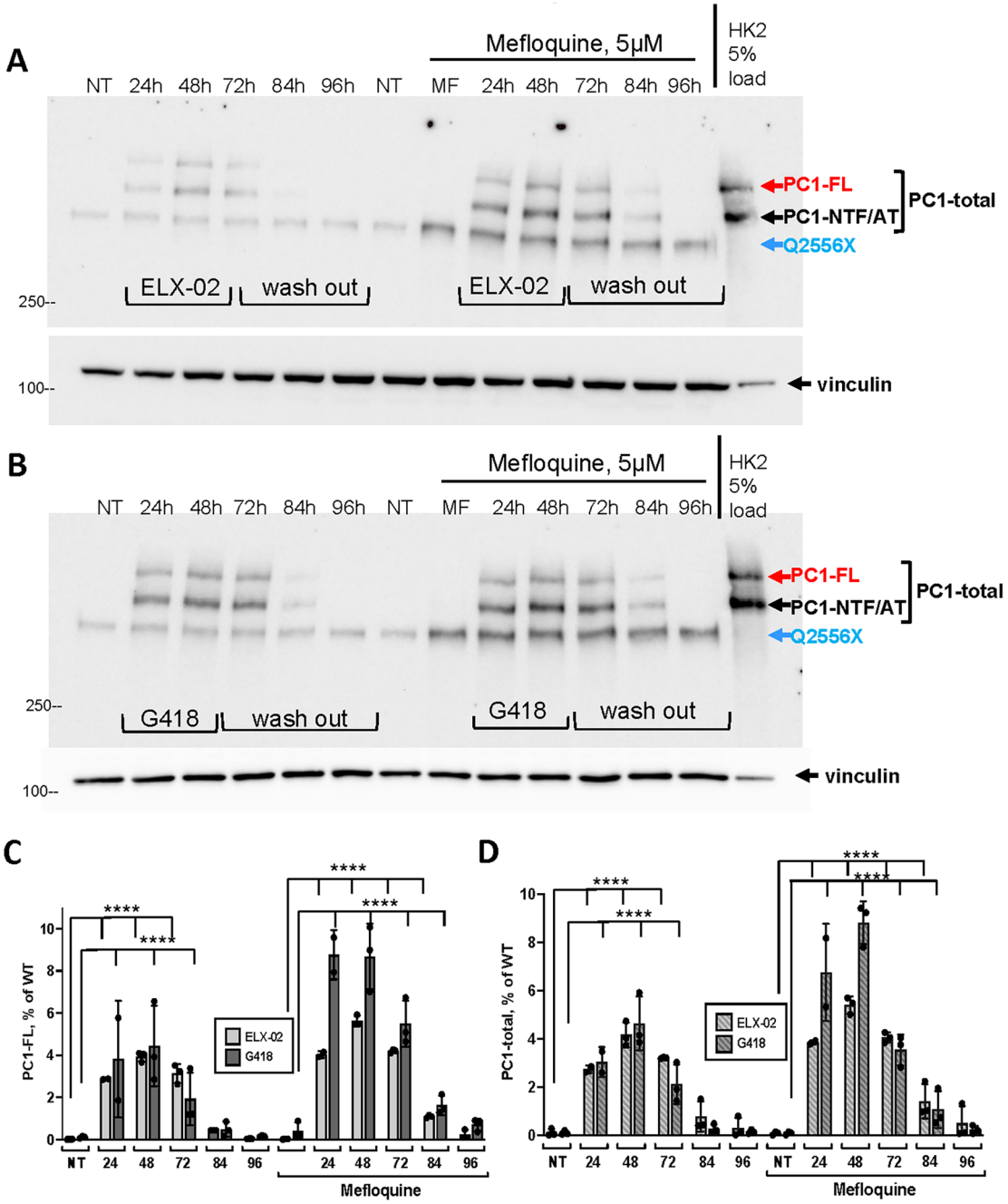

Fig. 5. Stability of AMG-mediated readthrough of endogenous PC1 protein from the *PKD1*-Q2556X allele in the patient-derived cells. (**A**) Mutant WT9-12 cells were treated with 400 μg/ml ELX-02 in the presence of absence of 5 μM mefloquine (MF) for 24–48 h, then washed and collected at 72, 84 and 96 h after the start of treatment. Please note that no ELX-02 was added in the lane labelled MF. (**B**) The cells were treated with 400 μg/ml G418 as in A. (**C**) Densitometric intensity of the full-length Polycystin1 (PC1-FL) band in three independent experiments was normalized to vinculin and presented as % of PC1-FL expression in wildtype HK-2 cells (last lane, 5% of loading comparing to the lysates from WT9-12 cells). (**D**) Densitometric intensity of the total Polycystin1 (combined PC1-FL and PC1-NTF/PC1-AT bands) in three independent experiments presented as % of PL1-total expression in wildtype cells. ****$p < 0.0001$. All samples were compared to the untreated sample (one way ANOVA) followed by the Tukey's multiple comparisons test. NT- nontreated cells; MF- mefloquine.

Recently, Vishy et al. reported that both ELX-02 and ELX-10 (the latter is a more recent modification of ELX compounds) reverse cystogenesis in iPSC-derived kidney organoids bearing bi-allelic *PKD1* and *PKD2* nonsense PTCs[45]. Intriguingly, despite a remarkable decrease in the percentage of cystic organoids, the authors detected low levels of full-length PC1 and virtually no expression of full-length PC2 in the ELX-treated mutant

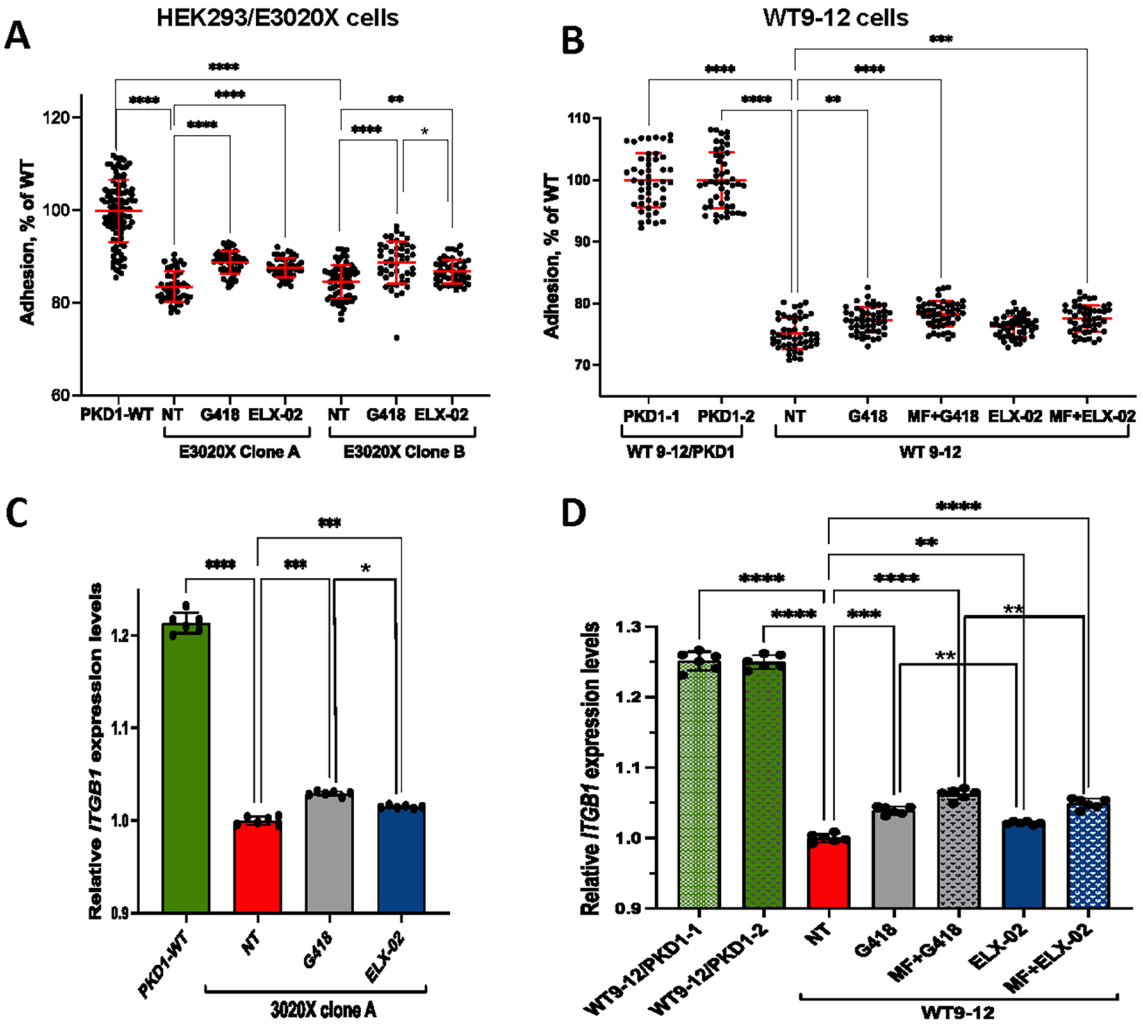

Fig. 6. Effect of aminoglycosides on cell adhesion. (**A**) HEK293 cells stably expressing PC1-E3020X-FLAG and matching control HEK293/PKD1-WT-FLAG clones were treated with 400 µg/ml ELX-02 or G418 for 48 h and then trypsinized. Equal number of cells was seeded in the 96-well plates coated with collagen 1 and allowed to adhere for 2 h. The intensity of the crystal violet-stained cells was measured. Intensities of all samples were normalized for the average intensity of the cells expressing PKD1-WT-FLAG. (**B**) Similar adhesion test was performed on WT9-12 cells bearing Q2556X pathogenic allele or matching WT9-12 clones stably expressing PKD1-WT-FLAG. Both G418 and ELX-02 modestly yet significantly increase cell adhesion in treated vs untreated cells. (**C**) Relative expression of *ITGB1* gene in each cell group described in A measured by quantitative RT-PCR. Expression in the untreated HEK293/PKD1-E3020X-FLAG cells is assigned "1" and the expression of other samples is normalized to the expression in untreated cells. (**D**) qRT-PCR measurements of relative *ITGB1* expression in the untreated WT9-12 cells (assigned "1"), treated mutant cells and WT9-12 clones stably expressing PKD1-WT-FLAG. Three independent experiments were carried out for each cell line. *$p \le 0.05$, **$p \le 0.01$, ***$p \le 0.001$ and ****$p \le 0.0001$. All samples were compared with one way ANOVA followed by the Tukey's multiple comparisons test. NT- nontreated cells; MF- mefloquine.

organoids. These unexpected results suggest that either the detection method was not sufficiently robust or that even a small, barely detectable, increase in expression of PC1 and PC2 levels might be sufficient to improve the cystogenic phenotype. To prove the latter point, the authors reported that ELX treatment of PC2 mutant organoids dramatically increased *PKD1* mRNA expression, even in the absence of detectable PC2 readthrough product[45], suggesting that low levels of polycystins can bring about impressive changes at the cellular level. By optimizing the Western immunodetection method, we improved detection of various PC1 forms. This allowed us to correlate PC1 levels with improvement in cell adhesion and signaling in aminoglycoside-treated mutant cells. Importantly, all assays in mutant WT9-12 cells measured the impact of de novo functional PC1 expression from only one Q2556X allele. Thus, clonal cysts in which a second allele bears a PTC could be highly sensitive to readthrough therapies.

Cells with inactivation of *PKD1* and *PKD2* are characterized by changes in cell adhesion, extra-cellular matrix composition or modification of integrin expression and signaling[26,28,29,47]. Castelli et al. reported that adhesion of canine medullary collecting duct, MDCK, cells overexpressing wildtype PC1 was more robust than

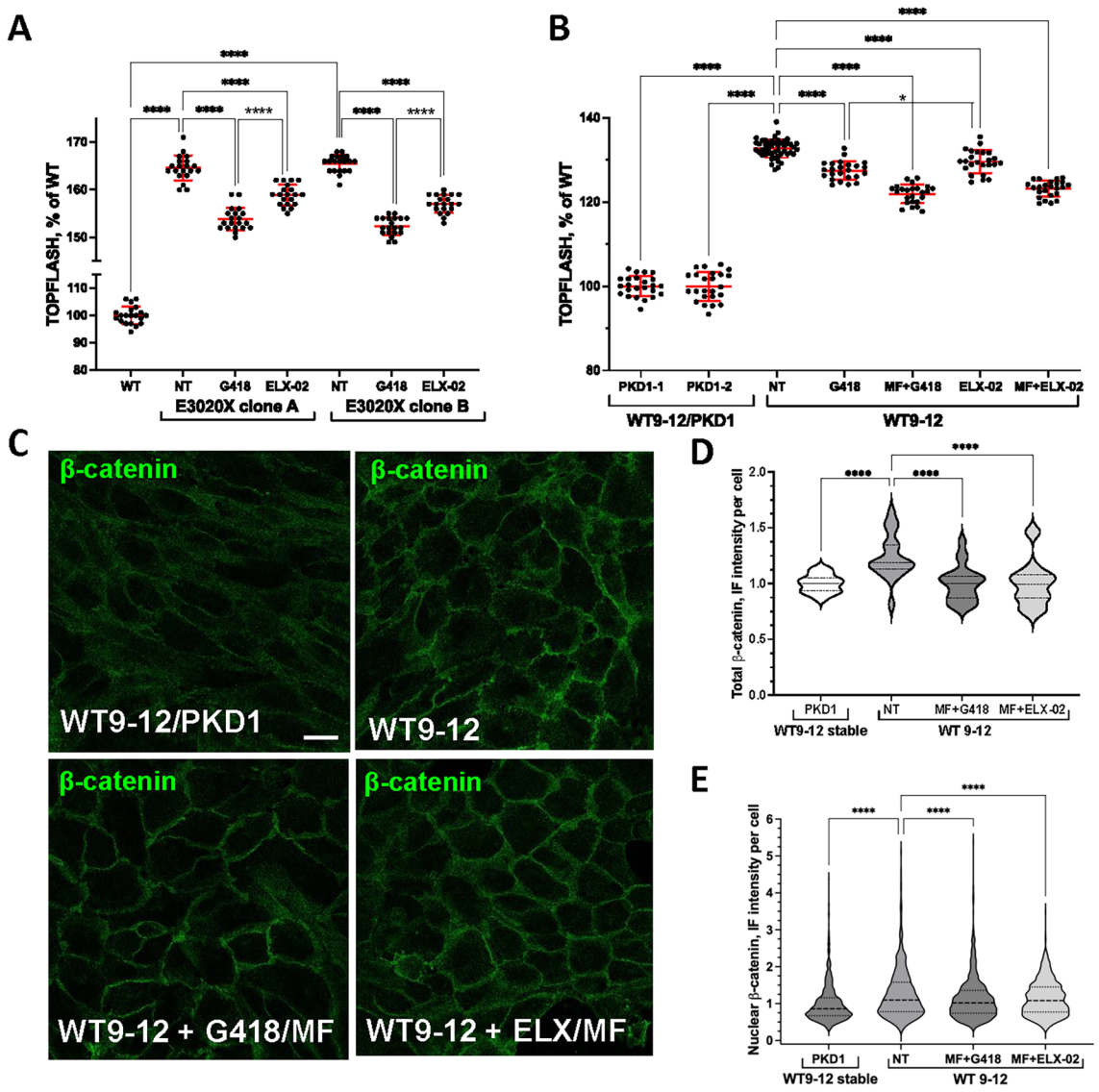

Fig. 7. Effect of aminoglycosides on WNT signaling in the *PKD1* PTC-bearing cells. (**A**) HEK293 cells stably expressing exogenous PKD1-WT-FLAG or PKD1-E3020X-FLAG constructs were transiently transfected with TOPFLASH reporter and Renilla luciferase to monitor transfection efficiency. The cells were treated with 400 μg/ml G418 or 400 μg/ml ELX-02 for 48 h, and half the samples were stimulated with the conditioned medium collected from L-WNT3a cells (ATCC) while the other half was treated with the conditioned medium from L cells (no WNT3, unstimulated cells) in the last 24 h. Luciferase activity in each sample was first normalized for transfection efficiency and then presented as a fold change in the WNT3a-stimulated vs non-stimulated cells. The fold change in the AMG untreated cells was considered as 100%, and all other variants were expressed as a percentage of the 100% in the untreated cells. (**B**) WT9-12 cells were transfected with TOPFLASH reporter, treated with aminoglycosides for 48 h and stimulated with WNT3a during the last 24 h. (**C**) Immunofluorescence detection of the β-catenin. WT9-12 cells were stably transfected with wildtype PKD1 expression construct, and the clones with the physiological levels (compared to the human proximal tubule cells HK-2) were chosen. These cells served as control. Scale bar is 20 μm. (**D**) Quantification of total β-catenin IF intensity in the WT9-12/PKD1 and WT9-12 cells treated with 400 μg/ml G418 or ELX-02 in the presence of mefloquine to maximize re-expression of functional PC1. (**E**) Quantification of the nuclear intensities of β-catenin, which is associated with higher WNT activity. Three independent experiments were carried out for each panel. *$p \leq 0.05$, ****$p \leq 0.0001$. One way ANOVA followed by the Tukey's multiple comparisons test. NT-nontreated cells; MF- mefloquine.

in the paternal MDCK clones, while adhesion of *Pkd1*−/− mouse fibroblasts was reduced comparing to control *Pkd1*+/+ cells[26]. The authors linked changes in adhesiveness to the changes in turnover of focal adhesions. β1-integrin, an important constituent of focal adhesions, and its downstream signaling pathways were elevated in mouse *Pkd1*−/− cells[28]. This suggests that the β1-integrin pathway is cystogenic. Similar observations were recently reported by Lichner et al.: porcine proximal tubule (LLCPK) cells with RNAi-mediated silencing of

Pkd1 or *Pkd2* genes expressed increased levels of *Itgb1* mRNA[29]. The results of our experiments are consistent with the model of *PKD1* overexpression reported by Castelli et al. Our HEK293/PKD1-WT-FLAG clones and WT9-12/PKD1-WT-FLAG clones exhibited increased cell adhesion to collagen I when compared to HEK293/PKD1-E3020X or mutant WT9-12 cells, similar to the MDCK cells overexpressing full-length wildtype PKD1 construct, reported by Castelli. Surprisingly, we also detected increased *ITGB1* mRNA expression in the control cells. The latter results contradict the observations by Lee and Lichner and are likely the consequence of wildtype PC1 overexpression in the cells that were used as control. Despite this limitation, both cell models expressing mutant *PKD1* PTC variants were informative for testing the effects of aminoglycosides. After aminoglycoside treatment, HEK293/PKD1-E3020X cells and WT9-12 cells displayed significantly enhanced adhesion and increased *ITGB1* mRNA expression, more closely resembling cells with wildtype PC1 expression. Remarkably, these changes parallelled the efficacy of aminoglycosides on *PKD1* PTC readthrough: G418 was more efficient than ELX-02 in enhancing adhesion/*ITGB1* mRNA expression, which was further potentiated by addition of mefloquine; the percentage increase in adhesion/*ITGB1* expression was consistent with the percentage of full-length PC1 readthrough in both cell models. The readthrough PC1 in the aminoglycoside-treated mutant WT9-12 cells reached plasma membrane surface, suggesting that it is a functional protein. Thus, we conclude that the changes in cell behavior were likely triggered by the de novo synthesis of full-length Polycystin1 induced by AMG treatment.

A hallmark of cyst formation in the *PKD1* and *PKD2* mutant models is the deregulation of multiple signaling pathways[32,48,49]. In this study, we show that treatment with aminoglycosides reduces inappropriately elevated transcriptional activity of both WNT and YAP signaling pathways in the *PKD1* mutant cells by decreasing nuclear localization and transcriptional activity of β-catenin and YAP, respectively. Importantly, the percentage improvement correlated with levels of full-length PC1 expression and was consistent with the higher potency of G418 compared to ELX-02.

Our study has several limitations. Although we interrogated the three existing types of STOP codons, it was done in various settings. This did not allow us to compare the efficacy of AMG-mediated readthrough on different types of PTCs. Also, we did not explore the nucleotide surroundings, proximity to the N-terminus or to exon–intron junctions; these parameters are known to contribute to the effectiveness of readthrough[50–52]. The human *PKD1* gene is one of the largest genes; furthermore, there are six pseudogenes along much of its length, making *PKD1* gene editing challenging. This precluded us from generating a library of cell clones with various PTCs or producing isogenic controls with a rescued Q2665X variant. We detected a modest, albeit highly significant, 5–8% AMG readthrough activity in WT9-12 cells, precluding the use of biochemical methods (e.g. nuclear fractionation) to detect the differences in nuclear β-catenin or YAP retention between the untreated and treated cells. Despite these limitations, the results of our study were dependable and highly reproducible.

In summary, we report that the aminoglycosides, G418 and ELX-02, elicit consistent readthrough of STOP codons (PTCs) in human *PKD1* mRNA and partially correct several pathogenic features of mutant *PKD1* cells. These observations support the hypothesis that selected aminoglycosides +/− mefloquine can induce sufficient readthrough to ameliorate cystic renal disease in ADPKD patients bearing *PKD1* premature termination codons.

Materials and methods

Plasmids

Human full-length (amino acids 1–4303) wildtype PKD1-WT-FLAG and PKD1-E3020X-FLAG expression vectors were obtained from Addgene (AF20 and AF41, respectively; Addgene, Watertown, MA, USA). In both constructs, FLAG tag is expressed in-frame at the C-terminus. The *PKD1* cDNA is expressed under CMV enhancer/promoter. The small FLAG-PKD1-NanoLuc and FLAG-PKD1-GFP reporters were custom-designed by GenScript (New Jersey, USA) by fusing in-frame a small fragment of the human *PKD1* gene encoding amino acids 4078–4303 with an N-terminally expressed FLAG tag and either a C-terminally expressed NanoLuc sequence (from pNLF1 vector, NCBI accession number KF811458) or eGFP sequence (from the GeneScript library). The matching FLAG-PKD1-R4228X-NanoLuc and FLAG-PKD1-R4228X-GFP reporters expressing common nonsense variant R4228X (C>T(12891, NCBI accession number NM_001009944.3) were also generated. All small reporters were made on the pcDNA3.1/Hygro(+) backbone from the GenScript library. Firefly Luciferase (pGL2-Empty control-SV40-Luc) was a gift from Rudolf Jaenisch (Addgene plasmid # 26280); Renilla Luciferase (R-Luc vector driven by the SV40 promoter, Promega, Car# E2231).

Cell culture and transfection

All experiments with human cells were covered by the Research Institute of the McGill University Health Centre Environmental Health and Safety protocol (230702-ET-1) and were conducted according to the institutional rules and regulations. The cells from the ATCC were obtained with the appropriate Material Transfer Agreements. Experiments were carried out in human embryonic kidney (HEK) 293 cells, human proximal tubule HK-2 cells (CRL-2190, ATCC, Manassas, VA, USA,) and WT9-12 cells (CRL-2833, ATCC). HEK293 cells were cultured in Dulbecco's modified Eagle's medium (DMEM, Wisent, St-Bruno, QC, Canada). HK-2 and WT9-12 cells were grown in a 1:1 mixture of DMEM and Ham's F12 medium (DMEM-F12, Wisent). All media were supplemented with 10% fetal bovine serum (FBS, heat-inactivated; Wisent), penicillin (100 units/ml) and streptomycin (100 µg/ml) both from Wisent. Cells were detached in 0.25% trypsin and 2.21 mM EDTA solution (Wisent). All cells were grown at 37 °C in a humidified environment at 5% CO_2.

Transfections were performed using jetPRIME reagent (VWR International, Mississauga, ON, Canada) according to the manufacturer's instructions. Small FLAG-PKD1-WT-GFP and FLAG-PKD1-R4228X-GFP reporters were transiently transfected using FuGENE®6 Transfection Reagent (Promega Corporation, E2691) according to the manufacturer's instructions. To generate stable clones, HEK293 cells were transfected with either the full-length PKD1-WT-FLAG or the PKD1-E3020X-FLAG construct, together with pcDNA3.1-hygro

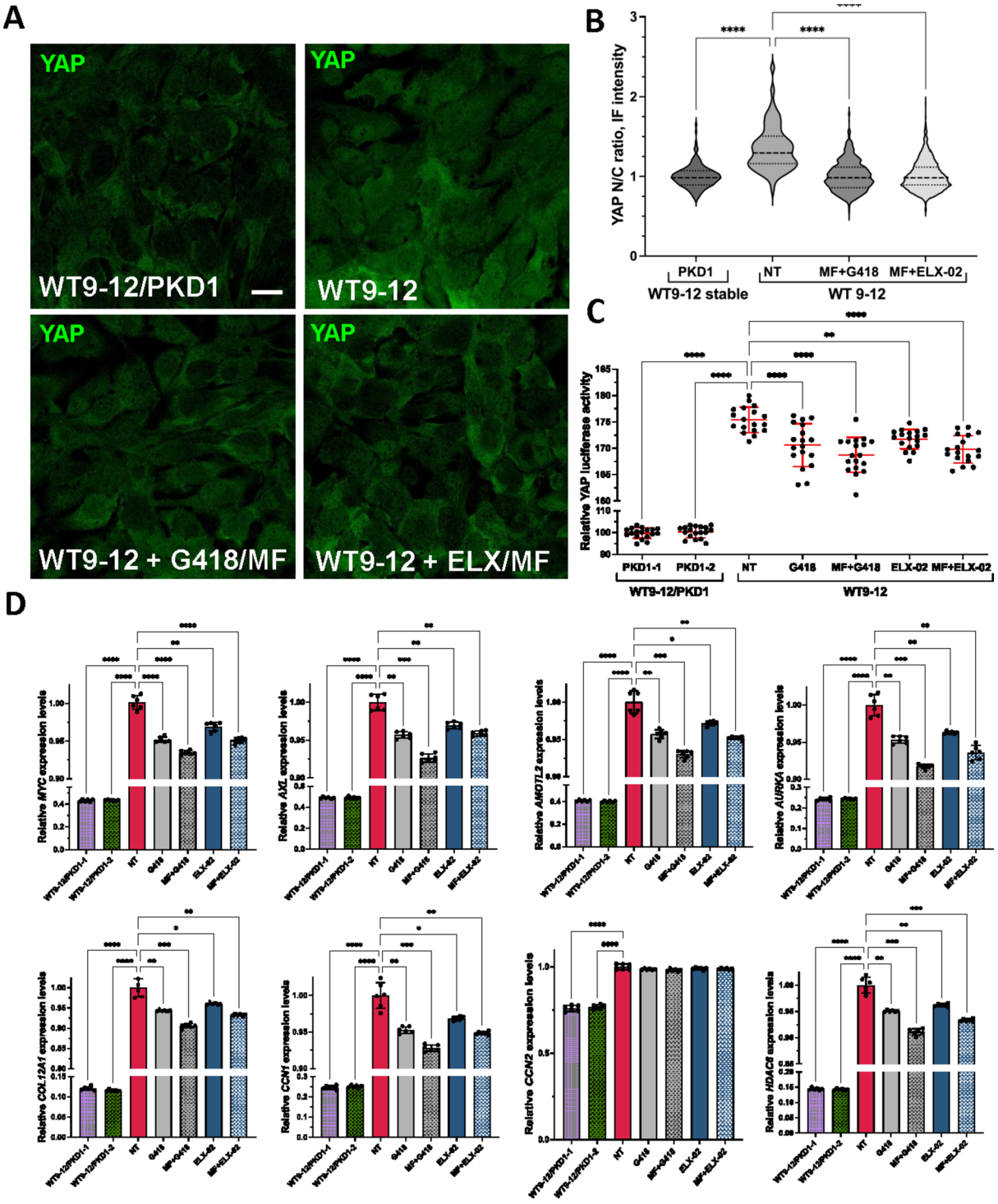

(Thermo Fisher, Waltham, MA, USA). The WT9-12 cells were transfected with the full-length PKD1-WT-FLAG and pcDNA3.1/Hygro (Invitrogen, Waltham, MA, USA). Forty-eight hours after transfection, cells were passaged, and individual clones were selected within three weeks in complete growth medium supplemented with hygromycin (0.3 mg/ml) (Thermo Fisher). The expression of exogenous wildtype or mutant Polycystin1 was confirmed by Western immunoblotting in several individual clones. The clones with the Polycystin1 expression at levels comparable to endogenous PC1 expression in the HK-2 cells were selected for further experiments.

Cell treatment with aminoglycosides

HEK293 clones stably expressing either full-length PKD1-WT-FLAG or PKD1-E3020X-FLAG, WT9-12 mutant cells, and WT9-12 cells stably expressing full-length PKD1-WT-FLAG protein were seeded in 24-well plates and treated 24 h later with 0–400 μg/mL ELX-02 (Eloxx Pharmaceuticals, USA), 0–400 μg/mL of G418 (Thermo Fisher), and/or 5 μM of mefloquine (Millipore Sigma, Oakville, ON, Canada) for 48 h. Control HK-2 cells were cultured alongside HEK293 and WT9-12 cells in the medium without drugs. In wash-off experiments, cells

◀**Fig. 8**. Effect of aminoglycosides on YAP signaling in the *PKD1* mutant cells. (**A**) Representative images of immunofluorescence detection of total YAP1 protein and its localization in the WT9-12 cells stably expressing wildtype PKD1-WT-FLAG (control) and in the mutant WT9-12 cells. The mutant cells were treated with 400 μg/ml G418 or ELX-02 +/− 5 μM mefloquine for 48 h. Scale bar is 20 μm. (**B**) Quantification of the nuclear/cytosolic ratio of YAP IF intensities. Nuclear YAP is associated with higher YAP signalling; cytosolic YAP is associated with inactive YAP. AMG treatment of the mutant cells leads to a partial decrease (~ 10%) of abnormal nuclear localization of YAP in the mutant cells. (**C**) WT9-12 cells and matching WT9-12 clones stably expressing wildtype PKD1-WT-FLAG construct were transfected with YAP-luciferase reporter, and the cells were treated with 400 μg/ml G418 or ELX-02 +/− 5 μM mefloquine. The luciferase activity was measured after 48 h of treatment. The AMGs significantly suppress YAP transcriptional signaling. (**D**) Quantitative RT-PCR to measure expression of YAP transcriptional targets. Relative expression of each gene in the untreated WT9-12 cells is assigned "1". Expression of each gene is normalized for its expression in untreated WT9-12 cells. Treatment with AMGs significantly lowers YAP target expression in 7/8 genes tested. Three independent experiments for each condition were carried out. Standard deviations are shown in all graphs. *$p \le 0.05$, **$p \le 0.01$, ***$p \le 0.001$, ****$p \le 0.0001$—samples were compared to the untreated sample (one way ANOVA followed by the Tukey's multiple comparisons test. NT—nontreated cells; MF—mefloquine.

were treated with aminoglycosides with or without mefloquine for 48 h, quickly washed and then switched to fresh medium without drugs. Cells were harvested or fixed, and assayed by Western blot, Luciferase assays, quantitative PCR and immunofluorescence as described below. To the HEK293 cells transiently transfected with small FLAG-PKD1-WT-Nanoluc, FLAG-PKD1-R4228X-Nanonluc, FLAG-PKD1-WT-GFP and FLAG-PKD1-R4228X-GFP, aminoglycosides and/or 7.5 μm mefloquine were added 6–8 h post-transfection, cells were cultured in the presence of drugs for 48 h and then processed for luciferase assays or GFP live imaging.

Western immunoblotting

Cell pellets were lysed on ice for twenty minutes in RIPA buffer (1 mM DTT, 1 mM EDTA, 1 mM EGTA, 150 mM NaCl, 50 mM Tris–HCl, pH 7.4, 1% Triton X-100) (all reagents from BioShop Canada, Burlington, ON, Canada), supplemented with 1 mM phenylmethylsulfonyl fluoride (PMSF, Millipore Sigma) and a complete protease inhibitor cocktail (Thermo Fisher). Cell lysates were centrifuged at 12,000*g* for 20 min at 4 °C, and the supernatants were stored at − 80 °C. Protein quantification was conducted using Bradford protein assay reagent (Bio-Rad, Mississauga, ON, Canada). Initially, we conducted a pilot study to optimize visualization of PC1 protein: various gel gradients, concentrations of sucrose and SDS were tested. Equal amounts of proteins per lane were separated on 4–10% polyacrylamide/0.2% SDS gels containing 6% sucrose and subsequently transferred to a nitrocellulose membrane (Bio-Rad) in 25 mM Tris, 192 mM glycine (Bioshop), and 20% methanol (Thermo Fisher). Blots were blocked in TBS (20 mM Tris–HCl, pH 7.5, and 137 mM NaCl) supplemented with 0.1% Tween 20 and 5% dried milk powder (reagents from Bioshop). Membranes were probed using mouse monoclonal antibodies against Polycystin1 (7E12, Santa Cruz, La Jolla, CA, USA), Flag M2 (Millipore Sigma), anti-GFP antibody (B2, Santa Cruz), and Vinculin (V9131, Millipore Sigma) followed by detection using Clarity™ Western ECL Substrate (Bio-rad) and ChemiDoc™ Imaging System (Bio-Rad). Densitometric analysis of protein expression levels was conducted via ImageJ[53], URL = http://imageJ. Three independent experiments per condition were carried out.

Real time quantitative reverse transcription—polymerase chain reaction

Total RNA was extracted with the RNeasy Plus mini kit (Qiagen Canada, Toronto, ON, Canada) in accordance with the manufacturer's instructions. The RNA concentration was quantified using a NanoDrop 2000c (Thermo Scientific, Waltham, MA, USA). RNA was reverse transcribed with SuperScript IV Vilo reverse transcriptase mastermix (Thermo Fisher) in accordance with the manufacturer's instructions. Quantitative real-time PCR (qPCR) was performed with SsoFast™ EvaGreen® Supermix (Bio-Rad) using the Applied Biosystems QuantStudio Real-Time PCR Detection System (Thermo Fisher). Results were calculated utilizing the ΔΔCt method. The level of gene expression in each sample was normalized to the reference human housekeeping HPRT gene and presented as a fold change relative to the expression of genes in cells untreated with aminoglycosides. Two biological replicas per experiment, three technical replicas per each biological sample were processed for each gene. A minimum of three independent experiments were carried out. The primer sequences utilized are listed in Supplemental Table.

Immunofluorescence

For all immunodetection experiments, cells were plated on cover slips coated with 15 μg/ml rat tail Collagen type I (Thermo Fisher) in a 12-well tissue culture plate (VWR International). Cells were treated for 48 h with aminoglycosides +/− mefloquine as described above, washed with PBS and fixed in 4% Paraformaldehyde (PFA)/PBS (Thermo Fisher) for 20 min at RT. For YAP1 and β-catenin immunodetection, the autofluorescence was quenched with 100 mM glycine in PBS for 10 min. Cells were permeabilized with 0.5% Triton X-100 (Fisher) in PBS for 5 min and then blocked for 30 min at room temperature in 10% Normal Donkey Serum (NDS) (Cedarlane, Burlington, ON, Canada), 1% Albumin Bovine Serum (BSA) (BioShop), 0.1% Triton X-100 in PBS. Cells were incubated with anti-YAP1 antibody (Cat# H00010413-M01, Abnova, Taipei, Taiwan) or anti-β-catenin antibody (Cat# 8480, Cell Signaling, Danvers, MA, USA) in 1% BSA, 0.1% Triton X-100 in PBS for 1.5 h at RT followed by incubation with secondary Donkey Alexa-488 anti-mouse IgG (H + L) antibody (Cat# A-21202, Thermo Fisher) or Donkey Alexa-488 anti-rabbit IgG (H + L) antibody (Cat# 711-545-152, Cedarlane)

in 5% NDS, 0.1% Triton X-100 in PBS for 1 h at RT. 4′,6-Diamidine-2′-phenylindole dihydrochloride (DAPI) (Millipore Sigma) was applied to stain nuclei, and the cells were mounted with Fluoromount-G™ Mounting Medium (Thermo Fisher). The images were captured on a LSM880 Laser Scanning Confocal Microscope (ZEISS, Oberkochen, Germany) using a Plan-Apochromat 63×/1.40 Oil DIC M27 lens. All images were analyzed by Zen 2.1 SP3 package software (ZEISS Blue edition) using Zones of Influence method; https://www.zeiss.com/microscopy/en/home.html?vaURL=www.zeiss.com/microscopy. The primary object was defined as the nucleus with the ZOI width 30 pixel around the nucleus. The area (μm^2) of each individual nucleus, the area of each ZOI and the mean intensity of YAP1 channel in each designated area were measured, and the ratio of nuclear YAP1 intensity per area unit to the intensity of YAP1 in the ZOI per area unit was calculated for each cell. Total β-catenin intensity per cell or per each nucleus was calculated using Image J. 10 images per experiment were taken in three independent experiments for YAP1 and β-catenin immunostaining.

GFP-expressing live-cell imaging

The HEK293 cells transiently transfected with small FLAG-PKD1-WT-GFP and FLAG-PKD1-R4228X-GFP reporters were treated with aminoglycosides for 48 h as described above. GFP expression in live cells was captured using transmitted light and a green fluorescence channel, objective X 10, on AxioObserver 100 inverted fluorescence microscope (ZEISS) using ZEN 2.6 software (ZEISS Blue Edition). The percentage of GFP-positive cells per image was calculated. The number of green + cells in the HEK293 cells expressing FLAG-PKD1-R4228X-GFP reporter was presented as a percentage of the green + HEK293 cells expressing wildtype FLAG-PKD1-WT-GFP, taken as "100%". A minimum of 10 images per experiment were captured; three independent experiments were carried out.

Cell adhesion assay

HEK293 clones stably expressing full-length PKD1-WT-FLAG or PKD1-E3020X-FLAG, WT9-12 cells and WT9-12/PKD1-WT-FLAG stable clones were treated for 48 h with 400 μg/mL aminoglycosides, +/− mefloquine, trypsinized, pelleted, and washed with DMEM. Cells were resuspended in DMEM/0.1% BSA, counted, and the concentration was adjusted to 500,000 cells/ml. 50,000 cells were seeded into each well of 96-well plates coated with 50 μg/ml of rat tail collagen type I (Cat# A1048301, Thermo Fisher) and incubated at 37 °C for 2 h. Control wells contained cell-free medium. The plates were then rinsed twice with ice-cold PBS on ice. Cells were fixed in cold methanol and stained for 10 min at RT with 0.5% crystal violet in 20% methanol. The wells were cleared with distilled water and air-dried overnight. 100 μl of 1% SDS solution was added to each well for 10 min at RT to solubilize the cells, and the absorbance was measured at 570 nm using an Infinite M200 Pro microplate reader (Tecan, Männedorf, Switzerland). The background for the staining procedure was measured at OD 570 in the wells without cells. Three independent experiments were carried out, 8 replicas per experiment for each condition.

Luciferase assay

HEK293 cells were transfected at 85–90% confluency with the small PKD1-WT-Nanoluc or PKD1-R4228X-Nanoluc reporters and a firefly luciferase reporter plasmid as an internal control at a ratio of 1:5. Six hours post-transfection, aminoglycosides and/or mefloquine were added to the medium. At 48 h, cells were collected, and nano-luciferase activity was quantified with the Nano-Glo luciferase assay (Promega, Madison, WI, USA) following the manufacturer's instructions. The assay for firefly luciferase was conducted according to manufacturer instructions (Pierce™ Renilla-Firefly Luciferase Dual Assay Kit (Thermo Fisher). YAP transcription activity was quantified utilizing the 8xGTIIc-luc (firefly) reporter (Cat# 34615, Addgene) alongside a Renilla-luciferase plasmid (10:1 ratio). At six hours post-transfection, fresh growth medium containing aminoglycosides, with or without mefloquine, was added and cells were collected at 48 h. To measure activity of canonical WNT signaling, a TOPFLASH construct[37] alongside a Renilla-luciferase construct was utilized; FOPFLASH reporter plasmid[37] with a mutant TCF/LEF binding site served as a negative control. Six hours post-transfection, aminoglycosides +/− mefloquine were added. At 24 h post-transfection, the medium was replaced with a 1:1 mixture of growth medium and conditioned medium (from L-Wnt3A cells or L-cells (CRL-2647 ™ and CRL-2648, respectively, ATCC) containing aminoglycosides. On the following day, cells were collected for assays. Firefly luciferase and Renilla luciferase activities were assessed using Pierce Renilla-Firefly Luciferase Dual assay kit (Thermo Fisher). Luciferase activities were measured using a Fluostar Optima luminometer (BMG Labtech, Ortenberg, Germany). Three technical replicas per condition per experiment were used; three independent experiments for each luciferase construct were conducted.

PrestoBlue cell viability assay

HEK293 and WT9-12 cells were seeded at a density of 0.03×10^6 cells per well in 48-well tissue culture plates and cultured in complete medium until ~ 85–90% confluency and then treated with aminoglycosides for 48 h, where indicated. PrestoBlue reagent (Thermo Fisher) was then added, and incubation was continued for 2 h. Absorbance was measured at 570 nm and normalized to the 600 nm value.

Cell surface biotinylation

We used the biotinylation method described in[54]. Briefly, WT9-12 cells were grown in 60 mm dishes, treated with aminoglycosides and mefloquine for 48 h as described above and rinsed twice with ice-cold PBS supplemented with 0.9 mM $CaCl_2$ and 0.49 mM $MgCl_2$ (pH 7.4) (Wisent). Cell surface proteins were biotinylated for 30 min by adding a 1 mg/ml solution of EZ-Link™ Sulfo NHS-LC-LC-Biotin (in supplemented PBS) (#A35358, Thermofisher) in the cold room. Biotinylation was stopped by three washes in cold 100 mM Glycine (pH 3.0) in supplemented PBS. Cells were then lysed in 1% Triton X-100, 150 mM NaCl, 10 mM Tris–HCl at pH 7.5,

1 mM EDTA, 1 mM EGTA, 0.5% NP-40, and 10% sucrose at 4 °C for 30 min. The lysates were collected by centrifugation at 15,000×*g* for 20 min, and biotin-labelled surface proteins were captured on NeutrAvidin Agarose beads (Pierce, Thermofisher) by rotating overnight at 4 °C. Proteins bound to beads were collected by a brief centrifugation at 3000×*g* for 1 min, and pellets were washed three times with lysis buffer for 20 min at 4 °C. Biotin-labeled surface proteins were eluted with SDS gel-loading buffer and analyzed by western blotting. Experiment was repeated twice.

Statistical analysis

GraphPad Prism software, version 10.6.1, https://www.dotmatics.com/ (La Jolla, CA) was used to produce all graphs and for statistical analyses. For two group comparisons, a two-tailed unpaired Student's t-test was used. For comparisons among more than two groups, one-way ANOVA was used followed by post-hoc analyses using Tukey's multiple comparisons test. The standard deviations are shown in all graphs. A p-value ≤ 0.05 was considered significant; the p-values in the graphs are * for $p \leq 0.05$, ** for $p \leq 0.01$, *** for $p \leq 0.001$, and **** for $p \leq 0.0001$; not significant values are not shown.

Data availability

All data are available upon request. Please contact Elena Torban at elena.torban@mcgill.ca or Paul Goodyer at paul.goodyer@mcgill.ca.

Received: 16 June 2025; Accepted: 30 October 2025
Published online: 22 November 2025

References

1. Chebib, F. T. et al. Autosomal dominant polycystic kidney disease: a review. *JAMA* (2025).
2. Cantero, M. D. R. & Cantiello, H. F. Polycystin-2 (TRPP2): Ion channel properties and regulation. *Gene* **827**, 146313 (2022).
3. Yoder, B. K., Hou, X. & Guay-Woodford, L. M. The polycystic kidney disease proteins, polycystin-1, polycystin-2, polaris, and cystin, are co-localized in renal cilia. *J. Am. Soc. Nephrol.* **13**(10), 2508–2516 (2002).
4. Nauli, S. M. et al. Polycystins 1 and 2 mediate mechanosensation in the primary cilium of kidney cells. *Nat. Genet.* **33**(2), 129–137 (2003).
5. Lavu, S. et al. The value of genotypic and imaging information to predict functional and structural outcomes in ADPKD. *JCI Insight* **5**(15), e138724 (2020).
6. Pirson, Y. Extrarenal manifestations of autosomal dominant polycystic kidney disease. *Adv. Chronic Kidney Dis.* **17**(2), 173–180 (2010).
7. Vlak, M. H. et al. Prevalence of unruptured intracranial aneurysms, with emphasis on sex, age, comorbidity, country, and time period: a systematic review and meta-analysis. *Lancet Neurol.* **10**(7), 626–636 (2011).
8. Mort, M. et al. A meta-analysis of nonsense mutations causing human genetic disease. *Hum. Mutat.* **29**(8), 1037–1047 (2008).
9. Li, C. & Zhang, J. Stop-codon read-through arises largely from molecular errors and is generally nonadaptive. *PLoS Genet.* **15**(5), e1008141 (2019).
10. Martin, R. et al. Aminoglycoside suppression at UAG, UAA and UGA codons in Escherichia coli and human tissue culture cells. *Mol. Gen. Genet.* **217**(2–3), 411–418 (1989).
11. Bidou, L. et al. Sense from nonsense: therapies for premature stop codon diseases. *Trends Mol. Med.* **18**(11), 679–688 (2012).
12. Omachi, K. et al. NanoLuc reporters identify COL4A5 nonsense mutations susceptible to drug-induced stop codon readthrough. *iScience* **25**(3), 103891 (2022).
13. Ferguson, M. W. et al. The antimalarial drug mefloquine enhances TP53 premature termination codon readthrough by aminoglycoside G418. *PLoS ONE* **14**(5), e0216423 (2019).
14. Yu, J. et al. Aminoglycoside stress together with the 12S rRNA 1494C>T mutation leads to mitophagy. *PLoS ONE* **9**(12), e114650 (2014).
15. Guan, M. X. Mitochondrial 12S rRNA mutations associated with aminoglycoside ototoxicity. *Mitochondrion* **11**(2), 237–245 (2011).
16. Sabbavarapu, N. M. et al. Exploring eukaryotic versus prokaryotic ribosomal RNA recognition with aminoglycoside derivatives. *Medchemcomm* **9**(3), 503–508 (2018).
17. Bidou, L. et al. Characterization of new-generation aminoglycoside promoting premature termination codon readthrough in cancer cells. *RNA Biol.* **14**(3), 378–388 (2017).
18. Kerem, E. ELX-02: an investigational read-through agent for the treatment of nonsense mutation-related genetic disease. *Expert Opin. Investig. Drugs* **29**(12), 1347–1354 (2020).
19. Gunn, G. et al. Long-term nonsense suppression therapy moderates MPS I-H disease progression. *Mol. Genet. Metab.* **111**(3), 374–381 (2014).
20. de Poel, E. et al. Functional restoration of CFTR nonsense mutations in intestinal organoids. *J. Cyst. Fibros* **21**(2), 246–253 (2022).
21. Ong, A. C. et al. Polycystin-1 expression in PKD1, early-onset PKD1, and TSC2/PKD1 cystic tissue. *Kidney Int.* **56**(4), 1324–1333 (1999).
22. Wei, W. et al. Characterization of cis-autoproteolysis of polycystin-1, the product of human polycystic kidney disease 1 gene. *J. Biol. Chem.* **282**(30), 21729–21737 (2007).
23. Nauli, S. M. et al. Loss of polycystin-1 in human cyst-lining epithelia leads to ciliary dysfunction. *J. Am. Soc. Nephrol.* **17**(4), 1015–1025 (2006).
24. Lea, W. A. et al. Human-specific abnormal alternative splicing of wild-type PKD1 induces premature termination of polycystin-1. *J. Am. Soc. Nephrol.* **29**(10), 2482–2492 (2018).
25. Wilson, P. D. et al. The PKD1 gene product, "polycystin-1," is a tyrosine-phosphorylated protein that colocalizes with alpha2beta1-integrin in focal clusters in adherent renal epithelia. *Lab Invest.* **79**(10), 1311–1323 (1999).
26. Castelli, M. et al. Regulation of the microtubular cytoskeleton by Polycystin-1 favors focal adhesions turnover to modulate cell adhesion and migration. *BMC Cell Biol.* **16**, 15 (2015).
27. Joly, D. et al. Beta4 integrin and laminin 5 are aberrantly expressed in polycystic kidney disease: role in increased cell adhesion and migration. *Am. J. Pathol.* **163**(5), 1791–1800 (2003).
28. Lee, K. et al. Inactivation of integrin-beta1 prevents the development of polycystic kidney disease after the loss of polycystin-1. *J. Am. Soc. Nephrol.* **26**(4), 888–895 (2015).
29. Lichner, Z. et al. Myocardin-related transcription factor mediates epithelial fibrogenesis in polycystic kidney disease. *Cells* **13**(11), 984 (2024).
30. Geng, L. et al. Identification and localization of polycystin, the PKD1 gene product. *J. Clin. Investig.* **98**(12), 2674–2682 (1996).

31. Huan, Y. & van Adelsberg, J. Polycystin-1, the PKD1 gene product, is in a complex containing E-cadherin and the catenins. *J. Clin. Investig.* **104**(10), 1459–1468 (1999).
32. Ma, M., Gallagher, A. R. & Somlo, S. Ciliary mechanisms of cyst formation in polycystic kidney disease. *Cold Spring Harb. Perspect. Biol.* **9**(11), a028209 (2017).
33. Lee, E. J. et al. TAZ/Wnt-beta-catenin/c-MYC axis regulates cystogenesis in polycystic kidney disease. *Proc. Natl. Acad. Sci. USA* **117**(46), 29001–29012 (2020).
34. Li, A. et al. Canonical Wnt inhibitors ameliorate cystogenesis in a mouse ortholog of human ADPKD. *JCI Insight* **3**(5), e95874 (2018).
35. Cai, J. et al. A RhoA-YAP-c-Myc signaling axis promotes the development of polycystic kidney disease. *Genes Dev.* **32**(11–12), 781–793 (2018).
36. Happe, H. et al. Altered Hippo signalling in polycystic kidney disease. *J. Pathol.* **224**(1), 133–142 (2011).
37. Veeman, M. T. et al. Zebrafish prickle, a modulator of noncanonical Wnt/Fz signaling, regulates gastrulation movements. *Curr. Biol.* **13**(8), 680–685 (2003).
38. Hayat, R., Manzoor, M. & Hussain, A. Wnt signaling pathway: A comprehensive review. *Cell Biol. Int.* **46**(6), 863–877 (2022).
39. Dupont, S. et al. Role of YAP/TAZ in mechanotransduction. *Nature* **474**(7350), 179–183 (2011).
40. Kolosova, O. et al. Mechanism of read-through enhancement by aminoglycosides and mefloquine. *Proc. Natl. Acad. Sci. USA* **122**(17), e2420261122 (2025).
41. Smith, J. E. & Baker, K. E. Nonsense-mediated RNA decay–a switch and dial for regulating gene expression. *BioEssays* **37**(6), 612–623 (2015).
42. Lindeboom, R. G. H. et al. The impact of nonsense-mediated mRNA decay on genetic disease, gene editing and cancer immunotherapy. *Nat. Genet.* **51**(11), 1645–1651 (2019).
43. Watnick, T. J. et al. Somatic mutation in individual liver cysts supports a two-hit model of cystogenesis in autosomal dominant polycystic kidney disease. *Mol. Cell* **2**(2), 247–251 (1998).
44. Cornec-Le Gall, E. et al. Genetics and pathogenesis of autosomal dominant polycystic kidney disease: 20 years on. *Hum. Mutat.* **35**(12), 1393–1406 (2014).
45. Vishy, C. E. et al. Genetics of cystogenesis in base-edited human organoids reveal therapeutic strategies for polycystic kidney disease. *Cell Stem Cell* **31**(4), 537-553.e5 (2024).
46. Anikster, Y. et al. Ocular nonnephropathic cystinosis: clinical, biochemical, and molecular correlations. *Pediatr. Res.* **47**(1), 17–23 (2000).
47. Zhang, Y., Reif, G. & Wallace, D. P. Extracellular matrix, integrins, and focal adhesion signaling in polycystic kidney disease. *Cell Signal.* **72**, 109646 (2020).
48. Richards, T., Wilson, P. & Goggolidou, P. Next generation sequencing identifies WNT signalling as a significant pathway in Autosomal Recessive Polycystic Kidney Disease (ARPKD) manifestation and may be linked to disease severity. *Biochim. Biophys. Acta Mol. Basis Dis.* **1870**(7), 167309 (2024).
49. Ma, M. et al. Loss of cilia suppresses cyst growth in genetic models of autosomal dominant polycystic kidney disease. *Nat. Genet.* **45**(9), 1004–1012 (2013).
50. Bonetti, B. et al. The efficiency of translation termination is determined by a synergistic interplay between upstream and downstream sequences in Saccharomyces cerevisiae. *J. Mol. Biol.* **251**(3), 334–345 (1995).
51. Mangkalaphiban, K. et al. Extended stop codon context predicts nonsense codon readthrough efficiency in human cells. *Nat. Commun.* **15**(1), 2486 (2024).
52. Lombardi, S. et al. Molecular insights into determinants of translational readthrough and implications for nonsense suppression approaches. *Int. J. Mol. Sci.* **21**(24), 9449 (2020).
53. Schneider, C. A., Rasband, W. S. & Eliceiri, K. W. NIH Image to ImageJ: 25 years of image analysis. *Nat. Methods* **9**(7), 671–675 (2012).
54. Qian, F. et al. Cleavage of polycystin-1 requires the receptor for egg jelly domain and is disrupted by human autosomal-dominant polycystic kidney disease 1-associated mutations. *Proc. Natl. Acad. Sci. USA* **99**(26), 16981–16986 (2002).

Acknowledgements

We would like to thank Zachary Sentell and Dr. Thomas Kitzler for help with NDM analysis of the PKD1 mutations.

Author contributions

L.C., S.B., N.K. C.F.C.—conducted investigation; L.C., P.R.G., E.T. —original draft preparation; L.C., P.R.G. and E.—data analysis, manuscript review and editing; P.R.G., A.A. and E.T.—project conceptualization; A.CM.O.—reagent supply, manuscript review and editing; E.T. and P.R.G.—supervision, manuscript writing and editing, funding acquisition. All authors have read and agreed to the published version of the manuscript.

Funding

This work is supported by the Department of Defence, USA, grant # W81XWH2010125 to PG and ET.

Declarations

Competing interests

The authors declare no competing interests.

Additional information

Supplementary Information The online version contains supplementary material available at https://doi.org/10.1038/s41598-025-26775-7.

Correspondence and requests for materials should be addressed to E.T. or P.R.G.